Marine Pollution Bulletin
April 2021, Volume 165 Pages 112116 (13p.)
https://doi.org/10.1016/j.marpolbul.2021.112116
https://archimer.ifremer.fr/doc/00679/79089/

Fate of floating plastic debris released along the coasts in a global ocean model

Chenillat Fanny [1, *], Huck Thierry [2], Maes Christophe [1], Grima Nicolas [2], Blanke Bruno [2]

[1] Laboratoire d'Océanographie Physique et Spatiale (UMR 6523 LOPS), Univ Brest, CNRS, IRD, Ifremer, IUEM, Plouzané, France
[2] Laboratoire d'Océanographie Physique et Spatiale (UMR 6523 LOPS), Univ Brest, CNRS, IRD, Ifremer, IUEM, Plouzané, France

* Corresponding author : Fanny Chenillat, email address : fanny.chenillat@univ-brest.fr

Abstract :

Marine plastic pollution is a global issue, from the shores to the open ocean. Understanding the pathway and fate of plastic debris is fundamental to manage and reduce plastic pollution. Here, the fate of floating plastic pollution discharged along the coasts is studied by comparing two sources, one based on river discharges and the other on mismanaged waste from coastal populations, using a Lagrangian numerical analysis in a global ocean circulation model. About 1/3 of the particles end up in the open ocean and 2/3 on beaches. The input scenario largely influences the accumulation of particles toward the main subtropical convergence zones, with the South Pacific and North Atlantic being mostly fed by the coastal population inputs. The input scenario influences the number of beached particles that end up in several coastal areas. Beaching occurs mainly locally, although a significant number of particles travel long distances, allowing for global connectivity.

Highlights

► Rivers and coastal populations are key sources of marine plastic pollution. ► This pollution accumulates at the coasts (~2/3) and on the open ocean (~1/3). ► Littering of coastal populations explains better the pollution of subtropical gyres. ► Floating debris can travel long distances (up to several thousand kilometers). ► Long-distance floating debris allows connectivity between remote coastal regions.

Keywords : Marine debris, Microplastics, Lagrangian analysis, Ocean surface pathways, Coastal pollution, Ocean connectivity

1. Introduction

Marine pollution from plastics is a global issue and challenge (persistence of plastics at sea, consequences for marine life and potentially human health) that infests the ocean from coastal regions (e.g., Bergmann et al., 2017; Napper and Thompson, 2020) to the open sea (Barnes et al., 2009; Law et al., 2010; Cozar et al., 2014; van Sebille et al., 2015; Lebreton et al., 2018). According to Geyer et al. (2017), about half of the plastic debris produced is less dense than seawater and, consequently, is expected to float at the sea surface. This floating pollution either accumulates in the center of subtropical gyres (e.g., the Pacific Garbage Patch) or is discharged onto coasts and beaches. Transport of plastic is affected by a variety of physical processes (van Sebille et al., 2020; Dobler et al., 2019) characterized by different temporal and spatial variability. The pathways and fate of plastic debris in the oceans are still uncertain for many reasons, including a misperception of their sources, both in terms of quantity and distribution (Viatte et al., 2020). Indeed, observations are still limited, and the origins of the plastic collected at sea and along coasts remain a challenge to identify or evaluate.

Most of the projects on this issue are nowadays oriented toward a particular region or theme (Black et al., 2020), whereas plastic pollution must be considered as a global concern (Maes et al., 2019). Understanding the main pathway and fate of plastic debris remains fundamental to better manage and reduce plastic pollution from an environmental and economic perspective. Indeed, Lau et al. (2020) have shown that if no plastic pollution reduction strategy is undertaken, plastic pollution will triple by 2040. Despite the multiplicity of plastic pollution sources and the large uncertainties about the contribution of land-based plastic pollution (Horton and Dixon, 2017), according to van Sebille et al. (2020), it is today recognized that coastal pollution is one of the largest sources of ocean plastic waste globally, with 5 to 12 million tons $year^{-1}$ (Jambeck et al., 2015). As estimated by Faris and Hart (1994), 80% of marine litter enters the ocean by land, with the remaining 20% assumed to come from marine activities

such as commercial and recreational fishing, cruises, and shipping (Lebreton et al., 2012). Given the scarcity of available data and observations on marine litter and plastic pollution (Galgani et al., 2021), numerical simulation can be used '*to fill in the gap' between these observations, and to test hypotheses about how plastic particles behave in the ocean*" as explained by van Sebille et al. (2020). Indeed, numerical models are proper tools for understanding the transport and dispersion of plastic in the ocean (Hardesty et al., 2017), especially in a Lagrangian framework (van Sebille et al., 2018).

For instance, Lebreton et al. (2012) studied the relative contributions of plastics from impervious watersheds, coastal population and shipping inputs to different accumulation zones. In their study, they estimated that between 28% and 40% of the released particles were beached, depending on the input scenario.

Using a similar numerical methodology, we study hereafter the fate of floating plastic pollution in the ocean as discharged along the coasts. We compare two different source scenarios in the global ocean: one based on river inputs, and the other based on population density along the coasts and waste management. We use a Lagrangian numerical analysis in conjunction with surface currents from a reanalysis of a global ocean circulation model with a horizontal resolution of 1/12˚. We discuss how the use of different scenarios helps to understand ocean connectivity and plastic pollution on a global scale. This study highlights the importance of considering accurate coastal inputs or sources, in particular littering from coastal populations, and provides insight into future strategies for monitoring and mitigating plastic debris. This study fits well within the main research priorities on marine plastic litter raised by the scientific community (Maximenko et al., 2019), in response to the G7 Science Ministers meeting in Berlin in October 2015 (Williamson et al., 2016), such as *understand the pathways* "establishing connections between sources and sinks for different types of debris", and *understand the sinks*, "including accumulation in remote locations". Section 2 presents the material and methods. Results for particles ending up at sea and in the convergence zones are given in section 3, whereas the specific analysis of particles ending up along the coast (beaching) is presented in section 4. Section 5 is the concluding section.

2. Material and methods

2.1. Global surface ocean circulation model

For this study, we use the sea surface current from the Global Ocean General Circulation Model GLORYS12V1, a leading global reanalysis of ocean circulation and physics (Lellouche et al., 2018). This reanalysis is part of the Copernicus Marine Environment Monitoring Service (CMEMS) with a new global eddy-resolving resolution and an ocean model with 50 vertical levels. The model component is the NEMO platform, forced at its surface by the ERA-Interim atmospheric reanalysis of the European Center for Medium-range Weather Forecast. These products are part of international efforts to give a better estimate of the global state of the oceans (von Schuckmann et al., 2016). This reanalysis covers the 1993-2018 altimetry era with a daily frequency, and provides not only a higher horizontal resolution compared to previous versions, but also improvements and corrections (Lellouche et al., 2018). In the following, we use the daily mean surface currents from the upper layer of the model with a thickness of 1 m, from 1 January 1993 to 31 December 2015 (GLOBAL REANALYSIS PHY_001_030 product downloaded from https://resources.marine.copernicus.eu). The products of the Copernicus reanalysis being provided on a regular grid (A-grid in the classification of Arakawa and Lamb (1977)), we interpolated the velocities on the ORCA 1/12° native C-grid to run the Lagrangian experiments.

2.2. Coastal plastic source scenarios

In this study, we compare two distinct scenarios of coastal sources of plastic particles: one based on inputs from the world's main rivers and the other based on the coastal population (Fig. S1), which we will identify as the river scenario and population scenario hereafter.

The ***river scenario*** comes from the model developed by Lebreton et al. (2017). This global model of plastic inputs from rivers into the oceans is based on waste management, population density and hydrological information. It estimates that about 2 million tons of plastic waste

116 enters the ocean every year from 40,760 rivers. The 20 most polluting rivers are mainly located
117 along the western North Pacific and account for 71% of the total (Fig. 1). The North Indian and
118 North Atlantic basins account for 13% and 12% of the river inputs, respectively. Data were
119 downloaded from the global model inputs for annual midpoint estimates in Lebreton et al.
120 (2017) (data are available at figshare.com at doi:10.6084/m9.figshare.4725541).
121 The second scenario is that of mismanaged waste from the coastal population, which we we
122 refer to as the ***population scenario*** hereafter. This is actually a proxy of the mismanaged waste
123 released by the coastal population entering the ocean, as described in van Sebille et al. (2015):
124 it is computed as the human population within 200 km of the coast, scaled by the amount of
125 mismanaged plastic waste available to enter the ocean by country in 2010 (as referenced in
126 Jambeck et al. (2015) as 'mismanaged waste', based on the economic level of the countries)
127 In this scenario, plastic debris entering the ocean is more widely distributed (Fig. 1 and Fig. S1)
128 over 2633 coastal input positions. The west coast of the North Pacific accounts for 37% of the
129 total population's input, a relative contribution that is half that of the river input scenario. The
130 North Atlantic shorelines represent the second-highest source of plastic inputs with 21% of
131 total inputs (43% more than river inputs). The North Indian basin represents 18% of the total
132 input. The Eastern Pacific, South Atlantic (east and west) and the Mediterranean Sea represent
133 larger sources of plastic (5%, 5% and 10%, respectively) than in the river scenario (<1%, 1% and
134 <1%, respectively). Data were provided by Erik van Sebille (pers. comm., 2018) based on the
135 estimate of Jambeck et al. (2015) that 4.8-12.7 million tons of land-based plastic debris entered
136 the ocean in 2010, which is 2-6 times more than the river input on average.
137 Both scenarios are projected and discretized on our model grid. The finite number of total
138 particles released over the course of the experiment, and rounding to an integer number of
139 particles released each month in the source grid cells, reduces the effective number of source
140 points as follows. For the river scenario, the finite number of particles released each month
141 (20,000) reduces the effective number of source points to 522 grid cells (Fig. S1). There are very
142 large sources, with about 10 rivers releasing more than 500 particles per month (representing
143 altogether more than 58% of the total), with the Yangtze River peaking at about 5000 particles
144 (25% of the total). For the population scenario, out of the 2633 source points provided by Erik

van Sebille (pers. comm., 2018) on a 1°x1° grid, the finite number of particles released each month reduces the effective number of source grid cells to 1196 in our experiment (i.e., more than twice that of the river scenario). There are no sources as extreme as in the river scenario; the peak values are about 350 particles per month (barely 2% of the total), with 23 sources releasing more than 100 particles per month (representing altogether 19% of the total).
Our objective is to diagnose how differences in input scenarios affect the fate of floating plastic debris on a global scale. Thus, to make the two scenarios comparable, we choose to ignore the difference in the total amount of plastic mass released in each scenario. For simplicity, we also choose to ignore the temporal variability of coastal inputs in the two scenarios (e.g., river discharge depends on rainfall variability). Thus, we consider that an equivalent mean amount of plastic is released every month over the 23 years of simulation (1993-2015) from their coastal positions (see next section) in both scenarios (river and population).

2.3. Lagrangian analysis

To study the fate and pathway of floating plastic debris in the global ocean, we use a Lagrangian approach with the Ariane methodology (Blanke and Raynaud, 1997). As detailed in Maes et al. (2018) or Dobler et al. (2019), the Ariane tool has been used so that the numerical particles are horizontally advected by surface currents and do not experience vertical motion. The plastic input data for both scenarios were gridded on the ORCA native grid at a resolution of 1/12˚ at the nearest ocean grid point, i.e., each source point is associated with a single grid cell of the model. The initial positions of the particles are determined randomly within the grid cell. Note that the population density proxy data set was available at a resolution of 1˚x1˚; for this reason, some final positions on the 1/12˚ grid are not initialized exactly at the coast (as strictly defined by the land-sea mask of the model) but near the coast. Two experiments are run according to the coastal input scenario (see previous section) with equivalent total particle numbers: 5,589,080 particles for the river scenario, and 5,571,720 particles for the population scenario (the particle numbers are slightly different due to rounding to an integer number of particles released each month). About 20,000 particles are thus released each month during the 23-year

period from 1993 to 2015 (i.e., about 240,000 particles released per year). Particles released at close locations within the same grid cell are subject to turbulent, seasonal and interannual variability in the surface current that will lead to dispersion in their trajectories. The positions of the particles are recorded with a monthly frequency. There are no explicit sinks in our approach i.e., the released particles stay indefinitely at the surface in the model, still moving or stuck along the coasts.

2.4. Particle behavior

We have diagnosed that particles can experience a different fate depending on their position and trajectory in the ocean:

- *case a*: the particle leaves the coastline and travels within the ocean domain until the end of the experiment;
- *case b*: the particle leaves the coastline, travels in the open ocean but ends up along the coast: we will define these particles as “beached”;
- *case c*: the particle never leaves the coastline but rather travels alongshore;
- *case d*: the particle never leaves its initial grid cell. More precisely, the particle can barely move but never leaves the grid point associated to its initial position. Such behavior results from a conjunction between the initial positioning (indented coastline) and the dynamics (convergence), which creates unfavorable conditions for moving to another grid cell. Note that this behavior concerns a very small fraction of the initialized particles (<1%, see section 3) and will be considered as a “rare cases” category.

Note that, in absolute terms, cases b and c could refer to a similar category of beaching and thus to the same local pollution by plastic debris. However, we choose to distinguish these two cases because of the possible role of river mouth dynamics in such behavior.

3. Open ocean convergence zones

The particles are released continuously in both experiments. After a few years of Lagrangian advection, the particles have spread almost all over the global ocean, from the coast to the open ocean. Only a few regions remain free of particles: the Southern Ocean (due to the strong northward Ekman transport), the Atlantic and Pacific equatorial regions (due to the strong Ekman transport divergence), and the northern North Pacific and Chukchi Sea in the Arctic. Figure 2 represents what could be roughly observed in terms of relative surface plastic pollution from space at any given time. The two scenarios have similarities and differences (Fig. 2). In both scenarios, surface plastics cover a large portion of the ocean between 45˚S and 45˚N. Particles seem to accumulate in bays, gulfs and seas surrounded by high-flow rivers (river inputs) and densely populated coastlines (population inputs), e.g., in the Bay of Bengal, Gulf of Guinea and China Sea (Reisser et al., 2013; Hinojosa and Thiel, 2009; Collignon et al., 2012; Ryan, 2013), similarly in both scenarios. Other regions of accumulation are in the centers of the subtropical gyres, regions known as CVZ (Convergence Zones), where plastic accumulates through Ekman transport (Kubota, 1994; Maximenko et al., 2012; van Sebille, 2015), mainly in the North Pacific and South Indian basins. Concentrations differ strongly between scenarios in the South Atlantic, North Atlantic, South Pacific, and Arctic, but also in some coastal regions (e.g., off Europe and Brazil). Another difference between the scenarios is the lower concentration of particles in the equatorial Pacific and equatorial Atlantic in the river scenario compared to the population scenario. These discrepancies between the scenarios are only due to the relative input of particles (as the dynamics are the same in both experiments). Compared to the in situ observations (see figure 1 “standardized data” of van Sebille et al., 2015), the population scenario seems to show better agreement than the river scenario in terms of relative amplitude and global distribution of surface plastic debris, mostly because of the higher concentrations in the North Atlantic, South Atlantic and South Pacific CVZs. It should be mentioned that no scenario exactly satisfies the relative concentrations of particles in the different regions, especially since the syntheses of observations do not agree with each other. This might be due to the fact that particles inputs are more widely distributed along the coast in the population scenario than in the river scenario, as described in section 2.2.

To determine the origins of these discrepancies and to untangle the fate and pathways of the particles, now we modify the standard way of analyzing the fate of our particles. Instead of merely looking at the position of particles at time *t*, which mixes particles of different ages (such as Fig. 2), we choose to focus on the position of particles as a function of their age, i.e., the time elapsed since their release. We can thus follow a cohort of particle traveling from their release position to their final position (Fig. 3). For this section, we focus on particles from *case a*, i.e., particles ending up at sea. Since particles may be released at the same location at different times, they may experience different dynamics; thus, such an analysis provides much more consistent statistics on the plastic fate at the ocean surface. Figure 3 shows both the quasi-initial position of the particles (i.e., one month after their release at the coast), and their position after 22 years. The one-month-old particles have experienced one month of dynamics and are still relatively close to their release position: such a representation gives a good approximation of the initialization of particles in terms of position and concentration. It also ~~explicitly~~ illustrates the main input differences between the scenarios: with the exception of the tropical areas of the West Pacific and Northeast Indian Oceans, all other shores show significant differences. As explained in section 2b, the population scenario is more widely spread, especially in relation to the American, European and African population. ~~Most of the older particles, which have been drifting with the currents for 20 years, aggregate in the centers of the gyres (while a few others are still drifting in highly dynamical regions such as the Agulhas Current or between the subtropical region of the South Indian Ocean and the southwestern Pacific Ocean).~~ After drifting with the currents for 20 years, the particles aggregate in the center of the gyres (while others still drift in highly dynamical regions such as the Agulhas Current or between the subtropical region of the South Indian Ocean and the southwestern Pacific Ocean).

Figure 3 highlights the importance of sources for accumulation in CVZs and, specifically, the local influence of plastic pollution in the main gyres. By the term "local" we define the particles that originate and end in the same region, as defined in figure S2. Whereas the North Pacific and South Indian CVZs show quite similar concentrations and positions to the first order in both scenarios, the concentration of particles in the South Pacific, North and South Atlantic CVZs is much lower in the river scenario than in the population scenario. Indeed, the sources around

the latter basins are much lower in the river scenario (Fig. 1) indicating that particles have mostly a local origin in many regions: particles initialized in one region are likely to stay in this region (e.g., North and South Atlantic, Southeast Pacific and Mediterranean). Outside the CVZs, particle concentrations are much lower (e.g., Maximenko et al., 2012; Law et al., 2014). In all basins, there is a very intense divergence of particles around the equator, due to the poleward Ekman transport associated with trade winds, such that particles from a sub-basin (North or South) are very likely to remain in their region of origin. As already highlighted by Lebreton et al. (2012), (i) because there is little exchange between hemispheres across the equator (except in a few coastal regions), and (ii) because the particles are mostly released in the Northern Hemisphere in the river scenario, there are far fewer particles that end up in the South Atlantic and South Pacific gyres than in their Northern Hemisphere counterparts. In the Indian basin, however, there is a seasonal north-south flush of particles along the eastern boundary (van der Mheen et al., 2020).

In addition to the local contribution of plastic pollution in the main gyres, ~~there is a strong remote influence due to~~ there is also a remote contribution allowed by the connectivity between sub-basins. This connectivity depends on the strength and extent of the attraction basins (Froyland et al., 2014). To study this connectivity from coastal regions to the open ocean, we determine the temporal accumulation of particles in the main gyres (Fig. 4) and establish a connectivity matrix from the coastal inputs of particles - i.e., the initial position of the particles - to their final position at sea (Fig. 5) between the sub-regions defined in Fig. S2 (see also the mapped initial positions given in Figs. S3 and S4). To better capture the open-ocean signal of the particles attracted (Fig. 4), we limit the extension of the CVZs to their core - where particles accumulate over time (van Sebille et al., 2020) – and focus on the five main CVZs (see the colored boxes in Fig. 3). The slope of the curve indicates whether particles accumulate mostly in an attractive CVZ (positive slope), whether particles escape mostly from a leaky CVZ (negative slope), or whether an equilibrium is reached between sources and sinks in an attractive but still leaky CVZ (null slope). Sinks may represent particles that move to other regions or that beach. The rate at which a CVZ attracts particles provides an indication of the origin of the particles:

289 the faster the early rate, the younger the particles are, the less they travel (and vice versa for a
290 slower rate).

291 In both *river* and *population* scenarios, the *Indian* CVZ is the region where plastics accumulate
292 the most and very rapidly: in 10 years up to 5.0% and 5.9% accumulate in the river and
293 population scenarios, respectively, with concentrations that continue to increase up to 15 years
294 of simulation. This results from the multiplicity of large sources converging to the Indian basin
295 (see IND.S in Figs. 5, S3 and S4), from local sources (all Indian) to remote sources (from the
296 Pacific and Atlantic shores). This is in line with Lebreton et al. (2012) who found that in the
297 Indian CVZ, the main contributors are Southeast Asia/Indonesia, Africa and India. Overall, the
298 South Indian is the most heterogeneously and widely impacted region, with particles coming
299 from all origins with the population inputs (except the Mediterranean) and from all over the
300 North Pacific and South Atlantic with the river inputs (Fig. 5). In this case, the particles likely
301 crossed the equator, for instance between the South and the North Indian during the
302 intermonsoon season, as recently documented by van der Mheen et al. (2020). This result
303 contrasts with that of Lebreton et al. (2012) who identified the greatest diversity of particle
304 origins in the Southeast Pacific. This discrepancy might be due to differences in input scenarios.
305 Interestingly, the North Indian feeds the Southeast Pacific (Fig. 5). This connection has already
306 been documented as the surface “superconvergence” pathway linking the south Indian Ocean
307 to the subtropical south Pacific gyre through the Great Australian Bight (Maes et al., 2018).

308 The *North Pacific* is the second region where plastics are accumulating the most and very
309 rapidly. The North Pacific CVZ starts to significantly attract particles after 2 years of simulation
310 and accumulates approximately the same number of particles in both scenarios, up to ~4% in
311 about 5 years (Fig. 4). Particles traveled for 2 years from the Pacific and Indian shores before
312 ending up in the CVZ (see PAC.NE in Figs. 5, S3 and S4). An equilibrium is reached between
313 sources and sinks in the population scenario. However, in the river scenario, the equilibrium
314 shows a dip from year 7 to year 15 (i.e., 2000 to 2008), which is not observed in the population
315 scenario. This difference may be due to interannual variability in the dynamics linking one of
316 the sources to the CVZ. Indeed, in the river scenario, some of the sources involved in the
317 feeding of the North Pacific CVZ in the population scenario must be missing (e.g., from the

Eastern Pacific). Toward the end of the simulation, after 15 years (i.e., from 2008), there is a second increase in both scenarios, showing that the dynamics have favored the accumulation of common sources – i.e., from North Pacific or South Indian - in the North Pacific CVZ. Interestingly, the period 2000 to 2015 corresponds to a cool phase of the Pacific Decadal Oscillation (PDO) and a positive phase of the North Pacific Gyre Oscillation (NPGO). Such interannual variability is beyond the scope of this paper, but additional attention could be given to linking particle accumulation to different modes of climate indices in future research projects.

In the *South Atlantic,* there is a rapid accumulation of particles, followed by a slower increase over the rest of the simulation with the population scenario (Fig. 4), due to the larger sources all around the basin, mostly from Southeastern America (Figs. 3, S1 and S3). However, with river inputs, the particle concentration in the South Atlantic CVZ increases slowly over the whole period because particles come from very remote sources, from all over the Indian and NW Pacific (see ATL.S. in Figs. 5 and S4).

Accumulations in the *North Atlantic* CVZ vary significantly according to the input scenario, as in Lebreton et al. (2012). In the river scenario, very few particles accumulate, and an equilibrium of ~0.1% is rapidly reached (Fig. 4), with particles being attracted only from the local shores (see ATL.N in Fig. 5). In the population scenario, a maximum is rapidly reached (1% in less than a year), followed by a decrease and a further increase toward an equilibrium of ~1.1% in 5 years (Fig. 4). In this case, there is a clear balance between the sources (North and South Atlantic shores) and the open waters of the North Atlantic (Fig. 5), with the dispersion of particles from the core in the *North Atlantic* waters.

In the *South Pacific* CVZ, particles accumulate very slowly and the maximum concentration of about 0.1 and 1% is reached in 15 years (ten times slower than in the North Atlantic CVZ) with river and population inputs, respectively. This is consistent with Lebreton et al. (2012) who identified that “particles originating from South Atlantic and identified in the South Pacific Gyre took more than 15 years to make the journey”. In both scenarios, the locations of sources are similar, but the concentration of inputs from the Eastern and Southwestern Pacific shores is higher in the population scenario (see the PAC.SE position in Fig. 5), as in Lebreton et al. (2012).

In terms of open ocean pollution (particles in case a, ending at sea), we evaluate that 28% (~470,000 particles) have a local origin in the river scenario, against 49% (~1,200,000 particles) in the population scenario (these numbers are computed as the sum of the diagonal terms of the connectivity matrix, Fig. 5). Thus, the remaining portions of the particles have a remote origin (with our definition of regions), respectively 72% in the river scenario and 51% in the population scenario. The NW Pacific shores represent the largest source of pollution at sea in both scenarios (Fig. 1): particles reach mostly the South Indian ($4.5\ 10^5$ and $3.8\ 10^5$ particles, i.e., 8% and 6.8% of the released particles) and the NE Pacific ($4.0\ 10^5$ and $3.0\ 10^5$ particles, i.e., 7.2% and 5.4% of the released particles), then the South Atlantic ($6.0\ 10^4$ and $5.8\ 10^4$ particles, i.e., 1.1% and 1.0% of the released particles) (numbers are given for river and population inputs, respectively). Within these regions are the three main CVZ in terms of total number of particles in cores. The NW Pacific is also a significant source of local pollution with $1.9\ 10^5$ and $1.2\ 10^5$ particles (i.e., 3.4% and 2.2% of released particles) for the river and population inputs, respectively. The remaining number of particles ($3.7\ 10^4$ and $1.8\ 10^4$ particles, i.e., 0.7% and 0.3% of released particles) ends up in the South Pacific (E and W) and North Indian.

In summary, these results emphasize the importance of the input of coastal sources in the total accumulation and composition of the 5 CVZ, and the possible exchanges between these regions. Our results show similarities and differences with those of Lebreton et al. (2012) (see above for more details) who performed a similar analysis. Although we found the same 5 CVZ, one of the most divergent results is that they find that northern CVZs accumulate more particles than southern CVZs (~25% in Northern Hemisphere CVZs compared to ~10% in Southern Hemisphere CVZs), which is not our case (we find that 5% of the particles accumulate in Northern Hemisphere CVZs versus ~8% in Southern Hemisphere CVZs). This discrepancy may be due to differences in the input scenarios, the numerical tools (from surface current products to Lagrangian experiments), and the methodology (definition of regions). However, it remains difficult to validate the most realistic solution due to the lack of in situ observations in these regions, especially in the Southern Hemisphere.

In total, in both scenarios, CVZs do not attract more than 20% of the total particles released at the coast after a few years of simulation (Fig. 4). While the defined CVZs cover only a fraction of

the patches in the gyres, i.e., the core, we found that only 29/45% of the particles end up in the open ocean, away from the coast, for the river and population scenarios, respectively (Fig. 6). The majority of the particles thus end up along the coast, 71/55% respectively, and we now examine in detail the behavior of these beached particles.

4. Beaching

As noted in many previous studies (e.g., Maximenko et al., 2012; van Sebille et al., 2015), coastal deposit of plastic debris represents an important reservoir in the total budget. In the present estimation of the model dispersion, a significant proportion of the particles released at the coast does not end up in the open ocean (*case a*). Indeed, 36 and 43 % of them end up on beaches (*case b*) while 34 and 11 % travel alongshore (*case c*), in the river and population scenarios, respectively (Fig. 6). In total, 70% and 54% of the particles end up on the coasts (sum of *case b* and *case c*) in the river and population scenarios, respectively. This is in good agreement with Lebreton et al. (2019) who showed that 67% of the world's plastic washed up on the coasts. Note that a small proportion of particles, ~1%, do not move from the grid cell where they were released. Details on these categories are given hereafter. Overall, the broad spatial spreading of beachings along the coasts (Fig. 7) is not strikingly different between the two scenarios (except for a few areas), especially when compared to the very contrasted input functions (Fig. S1).

In terms of sources, in both scenarios, coastal pollution originates mainly from the NW Pacific, North Indian and North Atlantic shorelines, mainly because these are the main sources of particles (Fig. 6). In the population scenario, most of the particles released from the Mediterranean shores actually beached. Depending on the region, the balance of *open-ocean-fate* (*case a*) and *coastal-fate* (*case b and c*) is variable (Fig. S5). The following regions contribute more than 50% of the total coastal pollution, as diagnosed in *cases b* and *c*: North Indian (56%), NW and SE Pacific (70% and 96%), North Atlantic (93%) and Mediterranean (97%) with the river scenario; and NW Pacific (57%), North Atlantic (65%) and Mediterranean (96%) with the population scenario (Fig. S5).

The origin of the particles that accumulate along the coast is mostly local (Figs. 7, 8, S6 and S7), i.e., the initial and final positions are in the same region (this is also true for the particles that stay on the coast in *case c*, Fig. S8). In both scenarios, we estimate that 85% (~2,000,000 particles) of the beached particles have a local origin (this number is computed as the sum of the diagonal terms of the connectivity matrix, Fig. 8) likely due to coastal retention and coastal recirculation. That is especially true for the NW Pacific, North Indian and North Atlantic in both scenarios, and additionally for the Mediterranean in the population scenario. It is not surprising that in the river scenario, the positioning of local beaching pollution corresponds to the river areas, i.e., the Niger, the Amazon, the Ganges and rivers of the NW Pacific region (Mekong, Yangtze, etc.) (Figs. 7 and S6). Rivers also appear to be hotspots for particle retention on coasts (with 34% of particles in *case c*, Fig. 6 and S8). With regard to the population scenario, where sources are more widely distributed, beaching locations appear to be widespread along the shores and, to a lesser extent, even in divergent regions such as coastal upwelling areas like California, Peru or NW Africa (Fig. 7).

Coastal pollution is not, exclusively and totally, local, and the beaching process may in fact occur after a long distance traveled. In both scenarios, we find that ~27% of the beached particles traveled less than 500 km, ~66% between 500 km and 5000 km, and ~7% more than 5000 km (Fig. 9). This highlights the *shore-to-shore* connectivity between remote regions (Fig. 8 and S9). For example, particles from the NW Pacific, which is the main source of coastal pollution, can reach the Pacific, Indian or South Atlantic. Conversely, in the population scenario, particles from the Atlantic shores can reach the West Pacific, South Indian, and also Arctic shores. The Indian shores are also a source of beaching for older particles in the West Pacific, in both scenarios.

To summarize, the impact of local pollution on beaching is even greater with population inputs rather than with river inputs. This result deserves more attention and, because of uncertainties and gaps in the observations of plastic waste, it remains challenging to predict the sources and fate of plastics in coastal systems, as reported recently by Galgani et al. (2021). As for the particles at sea in the CVZs, the differences between the two scenarios appear mainly in the North Atlantic and SE Pacific, where the sources are very different (Fig. S1). In the North

Atlantic, river inputs tend to stay locally on the coast (mostly from the Amazon and Niger), whereas population inputs represent a high source of beached and offshore pollution (from Europe and North America). In the SE Pacific, this local pollution is represented by a significant proportion of offshore pollution with population inputs. The Mediterranean and NE Atlantic are largely affected by beaching and coastal retention (Fig. 6 and Fig. S8) with population inputs. Interestingly, these results highlight the disparity between regions in terms of plastic pollution: some regions are strongly affected by coastal pollution (e.g., the North Pacific), due to coastal retention and coastal recirculation, while others have a significant proportion of particles staying offshore (e.g., North Indian and NW Pacific). In contrast to local pollution, there are a significant number of beached particles that have traveled long distances in both scenarios and this study highlights the main pathways of plastic debris between coastal regions and their ability to travel long distances before ending up at the coast. Note that the geographic differences found in the final positions of the particles between the two scenarios are directly related to the location of the input sources and differences in concentration. Given these differences between the input scenarios, the particles may encounter different oceanographic features and dynamics that are likely to influence their final positions. However, the statistical robustness of our approach relies on the use of several million particles to diagnose the main pathways from initial positions to final positions, overcoming the effect of small scales. Moreover, in our simulations, the particles do not sink, whereas in reality, such old particles would most likely fall down the water column (Egger et al., 2020; Pabortsava and Lampitt, 2020) under the action of biology (biofouling, ingestion, or aggregation) (e.g., Kooi et al., 2017; van Sebille et al., 2020).

A qualitative comparison with global beaching patterns, as compiled for instance in the LITTERBASE database (https://litterbase.awi.de/litter, Tekman et al., 2018), generally shows relatively good agreement, except for some regions. For instance, the database reports no beachings along the east coast of Africa from Somalia to Mozambique, and along the coasts of Oman and Yemen, probably due to a lack of observations.

A striking difference between the 2 scenarios is the complete absence of beachings along the Pacific coast of South America. Coastal plastic and other debris reported along the Chilean coast

463 suggest that the river input scenario is not sufficient to supply plastic particles to the South
464 Pacific, and in this respect the population scenario is more satisfactory (as reported in
465 LITTERBASE from Thiel et al. 2003; Hinojosa and Thiel, 2009; Hinojosa et al., 2011; Thiel et al.,
466 2013; Miranda-Urbina et al., 2015, Hidalgo-Ruiz et al., 2018). Similarly, the 2 scenarios differ
467 greatly along the east coast of America, where the river scenario leads to almost no beaching
468 north of Florida. This is not the case in LITTERBASE, confirming once again the need for
469 population inputs. Beaching patterns around the Indian basin and along the West Pacific coasts
470 are not significantly different between the 2 scenarios, and are in good agreement with
471 previously published results (van der Mheen et al., 2020). Beaching patterns around Australia
472 (PAC. SW in Fig. 8) differ from the 2 scenarios and the population scenario is in better
473 agreement with recent studies (Galaiduk et al. 2020) with significant input from local and
474 northwest Pacific shores.
475
476 **5. Conclusions**
477
478 The aim of this study is to investigate the pathway and fate of floating plastic debris, a key issue
479 that remains fundamental to better manage and reduce plastic pollution. We diagnose the fate
480 of plastic pollution discharged along the coasts by comparing two different types of sources in
481 the global ocean: one based on rivers and the other on the population density along the coasts.
482 We use a Lagrangian numerical analysis (forward particle tracking) based on surface currents
483 from reanalysis of a global ocean circulation model with a resolution of 1/12˚. Our results
484 highlight the importance of the input scenario for the concentration of dispersed particles in
485 the open ocean, in specific subtropical convergence zones for instance, and the number of
486 particles beaching around oceanic basins, such as the Mediterranean Sea. The concentration of
487 particles at sea in certain convergence zones is particularly sensitive to the input scenario. More
488 precisely, population-related inputs are critical to feed convergence zones of the South Pacific
489 and North Atlantic. Connectivity between coastal sources and open ocean regions also indicates
490 that the Indian region is the most heterogeneous in terms of pollution with population-related
491 inputs. More generally, particles ending up at sea represent less than half of the particles

492 released (and less than 20 % in the convergence zones), whereas more than 50% end up at the
493 coast.
494 A large fraction of the total particles released ends up along the coast, between 54% in the
495 population scenario and 70% in the river scenario. The number of particles that beach in certain
496 areas also depends particularly on the input scenario, such as the European West Coast, the
497 Mediterranean Sea, and African East Coast with the population input. Rivers represent a large
498 source of local coastal pollution, probably due to the retention and recirculation of coastal
499 waters. Regardless the input scenario, some regions are more subject to offshore pollution such
500 as the South Atlantic and the NE Pacific, while others are more largely affected by coastal
501 pollution (beaching) such as the NW Pacific, North Atlantic and Mediterranean shores. We have
502 found that particles can travel up to several thousand kilometers, allowing remote connectivity
503 between coastal regions. This property is of interest for the application to other types of
504 floating pollution or any conservative biogeochemical properties, or viruses and pathogens.
505 Our study remains an idealized case from several aspects, and from our point of view, the main
506 approximations are the “oversimplified” beaching process and the related dynamical processes.
507 Indeed, beaching of plastics is a complex process that is strongly influenced by small-scale
508 coastal ocean dynamics (Isobe et al., 2014), and by the local morphology of the coastline
509 (Zhang, 2017). Including Stokes-drift, waves or tides can also influence the number of particles
510 stuck to the coast, and increase it by more than three times (Dobler et al., 2019). Another key
511 point is the definition that can be given to the term “beaching”. Using a 1/12˚ eddy-resolving
512 ocean model, our definition is purely probabilistic since we define as beached particles those
513 that are at a certain distance from the coast (i.e., one grid point) (as similar studies e.g., van der
514 Mheen et al. (2020)).
515 Although this study is still based on available scenarios for plastic sources, it provides new
516 insights on connectivity between regions, on offshore pollution with CVZ composition and on
517 coastal pollution in terms of beaching. There are many ways to add complexity to these
518 processes. Indeed, for the sake of simplicity, we have neglected many key factors such as the
519 temporal/seasonal variability of coastal inputs that could change with rainfall (e.g., Lebreton et
520 al., 2017; van der Mheen et al., 2020), and also the significant worldwide increase in plastic

inputs to the sea in relation to population growth and the rapid increase in plastic production (Ostle et al., 2019). We have also ignored the contribution of pollution from maritime inputs along shipping route or fishery activities (e.g., Lebreton et al., 2012). With the 1/12˚ eddy-resolving ocean model used, one might have expected to find particles crossing the Antarctic Polar Front and reaching the Southern Ocean (Fraser et al., 2018), but it is likely that the absence of extreme events and Stokes drift (driven by surface winds) does not allow such connectivity. Finally, we focus on floating debris that could experience vertical motion in response to physical or biological processes (van Sebille et al., 2020). It could be interesting to implement models that allow interaction with the marine ecosystem – e.g., processes such as ingestion by plankton and fish, sedimentation by biofouling (Kooi et al., 2017) which could represent an important sink for particles toward the deep ocean (van Sebille et al., 2020). Indeed, it has recently been documented by Egger et al. (2020) that we can find below the surface (5 m depth) to 2,000 meters about 56%-80% of what is seen at the surface.

Marine plastic pollution represents an increasing threat to the environment. Because of their serious detrimental effects on marine ecosystems (see examples in Napper and Thomson, (2020)) and given the huge cost of removing this pollution from beaches (e.g., Burt et al., 2020; Cruz et al., 2020; Napper and Thomson, 2020), it is today fundamental to understand the fate and pathway of marine plastic debris. Such studies are needed to better inform and guide the stakeholders involved in the reduction of plastic pollution and waste management decision makers. However, a consensus is needed among researchers and a major step forward will be to improve the quality of information available on beached marine debris, which would require standardization of data sets (e.g., reporting metrics and sampling methods) (Serra-Gonçalves et al., 2019; Galgani et al., 2021).

Acknowledgements

FC was supported by postdoctoral funding from CNRS/INSU. We thank gratefully Laurent Lebreton and Erik van Sebille for providing their data sets for the source scenarios.

References

Arakawa, A. and V.R. Lamb, 1977: Computational Design of the Basic Dynamical Process of the UCLA General Circulation Model. Methods Computational Physics, 17, 173-265. http://dx.doi.org/10.1016/B978-0-12-460817-7.50009-4

Barnes, D. K. A., F. Galgani, R.C. Thompson, and M. Barlaz, 2009: Accumulation and fragmentation of plastic debris in global environments. *Philosophical Transactions of the Royal Society B: Biological Sciences* 364, 1985–1998.

Bergmann, M., B. Lutz, M. B. Tekman, L. Gutow, 2017: Citizen scientists reveal: Marine litter pollutes Arctic beaches and affects wild life, Marine Pollution Bulletin, 125, 1–2, 535-540, https://doi.org/10.1016/j.marpolbul.2017.09.055.

Blanke, B., and S. Raynaud, 1997: Kinematics of the Pacific equatorial undercurrent: An eulerian and lagrangian approach from GCM results. J. Phys. Oceanogr., 27, 1038-1053.

Black J.E., D.E. Holmes and L.M. Carr, 2020: A Geography of Marine Plastics, *Irish Geography, Vol. 53, No. 1, DOI: 10.2014/igj.v53i1.1411.*

Brach, L., P. Deixonne, M.-F. Bernard, A. ter halle, 2018: Anticyclonic eddies increase accumulation of microplastic in the North Atlantic subtropical gyre. Marine Pollution Bulletin, 126:191-196, DOI: 10.1016/j.marpolbul.2017.10.077.

Cruz, C.J., J. J. Muñoz-Perez, M. I. Carrasco-Braganza, P. Poullet, P. Lopez-Garcia, A. Contreras, R. Silva, 2020: Beach cleaning costs, Ocean & Coastal Management, Volume 188, 105118, doi.org/10.1016/j.ocecoaman.2020.105118.

Collignon A, Hecq J, Galgani F, Voisin P, Collard F, et al., 2012: Neustonic microplastic and zooplankton in the North Western Mediterranean Sea. Mar. Pollut. Bull. 64: 861–864.

Cózar, A., F. Echevarría, J. I. González-Gordillo, X. Irigoien, B. Úbeda, S. Hernández-León, Á. T. Palma, S. Navarro, J. García-de-Lomas, A. Ruiz, M. L. Fernández-de-Puelles, and C. M. Duarte, 2014: Plastic debris in the open ocean. PNAS 2014 111 (28) 10239-10244, doi:10.1073/pnas.1314705111.

Dobler, D., T. Huck, C. Maes, N. Grima, B. Blanke, E. Martinez, F. Ardhuin, 2019: Large impact of Stokes drift on the fate of surface floating debris in the South Indian Basin. Mar. Pollut. Bull., 148, 148, 202-209, doi: 10.1016/j.marpolbul.2019.07.057.

Egger, M., Sulu-Gambari, F. & Lebreton, L. 2020: First evidence of plastic fallout from the North Pacific Garbage Patch. *Sci Rep* **10,** 7495. https://doi.org/10.1038/s41598-020-64465-8.

Faris, J., Hart, K., 1994: Seas of Debris: A Summary of the Third International Conference on Marine Debris. N.C. Sea Grant College Program and NOAA.

Froyland, G., R. M. Stuart, and E. van Sebille, 2014: How well connected is the surface of the global ocean? Chaos, 24, 033 126.

Galgani, F., Brien, A.So., Weis, J. *et al.*, 2021. Are litter, plastic and microplastic quantities increasing in the ocean?. *Micropl.&Nanopl.* **1,** 2. https://doi.org/10.1186/s43591-020-00002-8

Geyer, R., J.R. Lambeck, K. Lavender Law, 2017: Production, use, and fate of all plastics ever made. Science Advances, 3, 1-5, 19July2017.

Hardesty B D, Harari J, Isobe A, Lebreton L C M, Maximenko N A, Potemra J, van Sebille E, Vethaak A D and Wilcox C, 2017: Using numerical model simulations to improve the understanding of micro-plastic distribution and pathways in the marine environment. Front. Mar. Sci. 4:30, doi: 10.3389/fmars.2017.00030.

Hidalgo-Ruz, V., Honorato-Zimmer, D., Gatta- Rosemary, M., Nuñez, P., Hinojosa, I.A. and Thiel, M., 2018: Spatio-temporal variation of anthropogenic marine debris on Chilean beaches. *Marine Pollution Bulletin,* 126, 516–524. https:// doi.org/10.1016/j.marpolbul.2017.11.014.

Hinojosa I, Thiel M, 2009: Floating marine debris in fjords, gulfs and channels of southern Chile. Mar. Pollut. Bull. 58, 341–350.

Hinojosa, I. A., Rivadeneira, M.M., Thiel, M., 2011: Temporal and spatial distribution of floating objects in coastal waters of central–southern Chile and Patagonian fjords, Continental Shelf Research, 31, Issues 3–4, 172-186, doi.org/10.1016/j.csr.2010.04.013.

Isobe, A., Kubo, K., Tamura, Y., Kako, S., Nakashima, E., and Fujii, N., 2014: Selective transport of microplastics and mesoplastics by drifting in coastal waters, Marine Pollution Bulletin, 89, 324–330, https://doi.org/10.1016/j.marpolbul.2014.09.041.

Jambeck, J. R., R. Geyer, C. Wilcox, T. R. Siegler, M. Perryman, A. Andrady, R. Narayan, and K. L. Law, 2015: Plastic waste inputs from land into the ocean. Science, 347, (6223) 768-771, DOI: 10.1126/science.1260352.

Kooi M., E.H. van Nes, M. Scheffer and A.A. Koelmans, 2017: Ups and Downs in the Ocean: Effects of Biofouling on Vertical Transport of Microplastics. Environ. Sci. Technol., 51, 7963−7971. DOI: 10.1021/acs.est.6b04702.

Kubota, M., 1994: A Mechanism for the Accumulation of Floating Marine Debris North of Hawaii. J. Phys. Oceanogr., 24, 1059-1064, doi: 10.1175/1520-0485.

636 Lau W.W.Y, Y. Shiran, R.M. Bailey et al., 2020: Evaluating scenarios toward zero plastic
637 pollution. Science, 369, 6510, 1455-1461, DOI: 10.1126/science.aba9475.
638
639 Law K. L., S. E. Morét-Ferguson, D. S. Goodwin, E. R. Zettler, E. DeForce, T. Kukulka and G.
640 Proskurowski, 2014: Distribution of surface plastic debris in the Eastern Pacific Ocean from an
641 11-year data set. Environ. Sci. Technol. 48, 4732–4738.
642
643 Law K. L., S.E. Morét-Ferguson, N. A. Maximenko, G. Proskurowski, E. E. Peacock, J. Hafner and
644 C. M. Reddy, 2010: Plastic accumulation in the North Atlantic subtropical gyre. Science, 329
645 1185–1188.
646
647 Lebreton, L.C.M., S. Greer, and J. Borrero, 2012: Numerical modelling of floating debris in the
648 World's Ocean. Mar. Pollut.Bull., 64, 653-661.
649
650 Lebreton, L.C.M, B. Slat, F. Ferrari, B. Sainte-Rose et al., 2018: Evidence that the Great Pacific
651 Garbage Patch is rapidly accumulating plastic, Nature Scientific report, *8:4666,*
652 DOI:10.1038/s41598-018-22939-w.
653
654 Lebreton, L.C.M., J. van der Zwet, J.-W. Damsteeg, B. Slat, A. Andrady, J. Reisser, 2017: River
655 plastic emissions to the world's oceans. Nature Communications, 8, 15611, DOI:
656 10.1038/ncomms15611.
657
658 Lellouche, J.-M.; Greiner, E.; Le Galloudec, O.; Garric, G.; Regnier, C.; Drevillon, M.; Benkiran,
659 M.; Testut, C.-E.; Bourdalle-Badie, R.; Gasparin, F.; et al., 2018: Recent updates to the
660 Copernicus Marine Service global ocean monitoring and forecasting real-time 1/12 high-
661 resolution system. Ocean Sci., 14, 1093–1126, https://doi.org/10.5194/os-14-1093-2018.
662
663 Maes, C., and B. Blanke, 2015: Tracking the origins of plastic debris across the Coral Sea: A case
664 study from the Ouvéa Island, New Caledonia. Mar. Pollut. Bull., 97, (1-2) 16-168.

Maes, C., N. Grima, B. Blanke, E. Martinez, T. Paviet-Salomon, T. Huck, 2018: A surface "super-convergence" pathway connecting the South Indian Ocean to the subtropical South Pacific gyre. Geophysical Research Letters, 45, (4) 1915-1922, 2017GL076366, doi: 10.1002/2017GL076366.

Maes T., J. Perry, K. Alliji, C. Clarke, S.N.R. Birchenough, 2019: Shades of grey: Marine litter research developments in Europe, Marine Pollution Bulletin, 146, 274-281, DOI: 10.1016/j.marpolbul.2019.06.019.

Maximenko, N.A., J. Hafner, and P. Niiler, 2012: Pathways of marine debris from trajectories of Lagrangian drifters. Marine Pollution Bulletin, 65 (1-3), 51-62, doi:10.1016/j.marpolbul.2011.04.016.

Maximenko Nikolai, Corradi Paolo, Law Kara Lavender, Van Sebille Erik, Garaba Shungudzemwoyo P., et al., 2019: Toward the Integrated Marine Debris Observing System. Frontiers in Marine Science, 6, 447. DOI=10.3389/fmars.2019.00447

Miranda-Urbina, D., Thiel, M., Luna-Jorquera, G., 2015: Litter and seabirds found across a longitudinal gradient in the South Pacific Ocean, Marine Pollution Bulletin, Volume 96, Issues 1–2, Pages 235-244, doi.org/10.1016/j.marpolbul.2015.05.021.

Napper, I. E. and R. C. Thompson, 2020: Plastic Debris in the Marine Environment: History and Future Challenges. Global Challenges 4,1900081. DOI:10.1002/gch2.201900081.

Ostle, C., Thompson, R.C., Broughton, D. et al., 2019: The rise in ocean plastics evidenced from a 60-year time series. *Nat Commun* **10,** 1622. https://doi.org/10.1038/s41467-019-09506-1

Pabortsava, K., Lampitt, R.S., 2020: High concentrations of plastic hidden beneath the surface of the Atlantic Ocean. Nat Commun 11, 4073, doi: 10.1038/s41467-020-17932-9.

694
695 Reisser J, Shaw J, Wilcox C, Hardesty B, Proietti M, 2013: Marine plastic pollution in the waters
696 around Australia: Characteristics, concentrations and pathways. PloS one 8,
697 doi:10.1371/journal.pone.0080466.
698
699 Ryan, P.G., 2013: A simple technique for counting marine debris at sea reveals steep litter
700 gradients between the Straits of Malacca and the Bay of Bengal. Mar. Pollut. Bull. 69, 128–136,
701 doi: 10.1016/j.marpolbul.2013.01.016.
702
703 Serra-Gonçalves, C., Lavers, J. L., & Bond, A. L., 2019: Global Review of Beach Debris Monitoring
704 and Future Recommendations. *Environmental Science & Technology*, *53*(21), 12158–12167.
705 https://doi.org/10.1021/acs.est.9b01424
706
707 Tekman, M. B.; Gutow, L.; Macario, A.; Haas, A.; Walter, A.; Bergmann, M. 2018: LITTERBASE;
708 Alfred Wegener Institute for Polar and Marine Research: Bremerhaven, Germany, 2018.
709 http://litterbase.awi. de/interaction_detail (accessed September 2020).
710
711 Thiel, M., Hinojosa, I. A., Miranda, L., Pantoja, J. F., Rivadeneira, M. M., Vásquez, N., 2013:
712 Anthropogenic marine debris in the coastal environment: A multi-year comparison between
713 coastal waters and local shores, Marine Pollution Bulletin, 71, Issues 1–2, 307-316,
714 doi.org/10.1016/j.marpolbul.2013.01.005.
715
716 Thiel, M., Hinojosa, I., Vásquez, N., Macaya, E., 2003: Floating marine debris in coastal waters of
717 the SE-Pacific (Chile), Marine Pollution Bulletin, 46, Issue 2, 224-231, doi.org/10.1016/S0025-
718 326X(02)00365-X
719
720 van der Mheen, M., E. van Sebille, C. Pattiaratchi, 2020: Beaching patterns of plastic debris
721 along the Indian Ocean rim. Ocean Science Discussions, DOI: 10.5194/os-2020-50.
722

723 van Sebille E., 2015: The oceans' accumulating plastic garbage. Phys. Today, 68, 60–1.
724
725 van Sebille, E., M. H. England, and G. Froyland, 2012: Origin, dynamics and evolution of ocean
726 garbage patches from observed surface drifters. Environ. Res. Lett., 7, 044040, 6pp.
727 http://iopscience.iop.org/article/10.1088/1748-9326/7/4/044040.
728
729 van Sebille, E., C. Wilcox, L. Lebreton, N. Maximenko, B.D. Hardesty, J.A. Van Franeker, M.
730 Eriksen, D. Siegel, F. Galgani, and K. L. Law, 2015: A global inventory of small floating plastic
731 debris. Environ. Res. Lett., 10, 124006, 12pp, doi: 10.1088/1748-9326/10/12/124006 .
732
733 van Sebille, E., et al., 2020: The physical oceanography of the transport of floating marine
734 debris. Environmental Research Letters, 15, 023003, doi: 10.1088/1748-9326/ab6d7d.
735
736 Karina von Schuckmann, Pierre-Yves Le Traon, Enrique Alvarez-Fanjul, Lars Axell, et al.,
737 2016: The Copernicus Marine Environment Monitoring Service Ocean State Report, Journal of
738 Operational Oceanography, 9:sup2, s235-s320, DOI: 10.1080/1755876X.2016.1273446
739
740 Viatte, C., Clerbaux, C., Maes, C., Daniel, P., Garello, R., Safieddine, S., Ardhuin, F., 2020: Air
741 Pollution and Sea Pollution Seen from Space. Surv. Geophys., doi:10.1007/s10712-020-09599-0.
742 https://doi.org/10.1007/s10712-020-09599-0.
743
744 Williamson, P., Smythe-Wright, D., and Burkill, P., Eds., 2016: Future of the Ocean and its Seas:
745 a non-governmental scientific perspective on seven marine research issues of G7 interest. ICSU-
746 IAPSO-IUGG-SCOR, Paris.
747
748 Zhang, H., 2017: Transport of microplastics in coastal seas, Estuarine, Coastal and Shelf Science,
749 199, 74–86, https://doi.org/10.1016/j.ecss.2017.09.032.
750

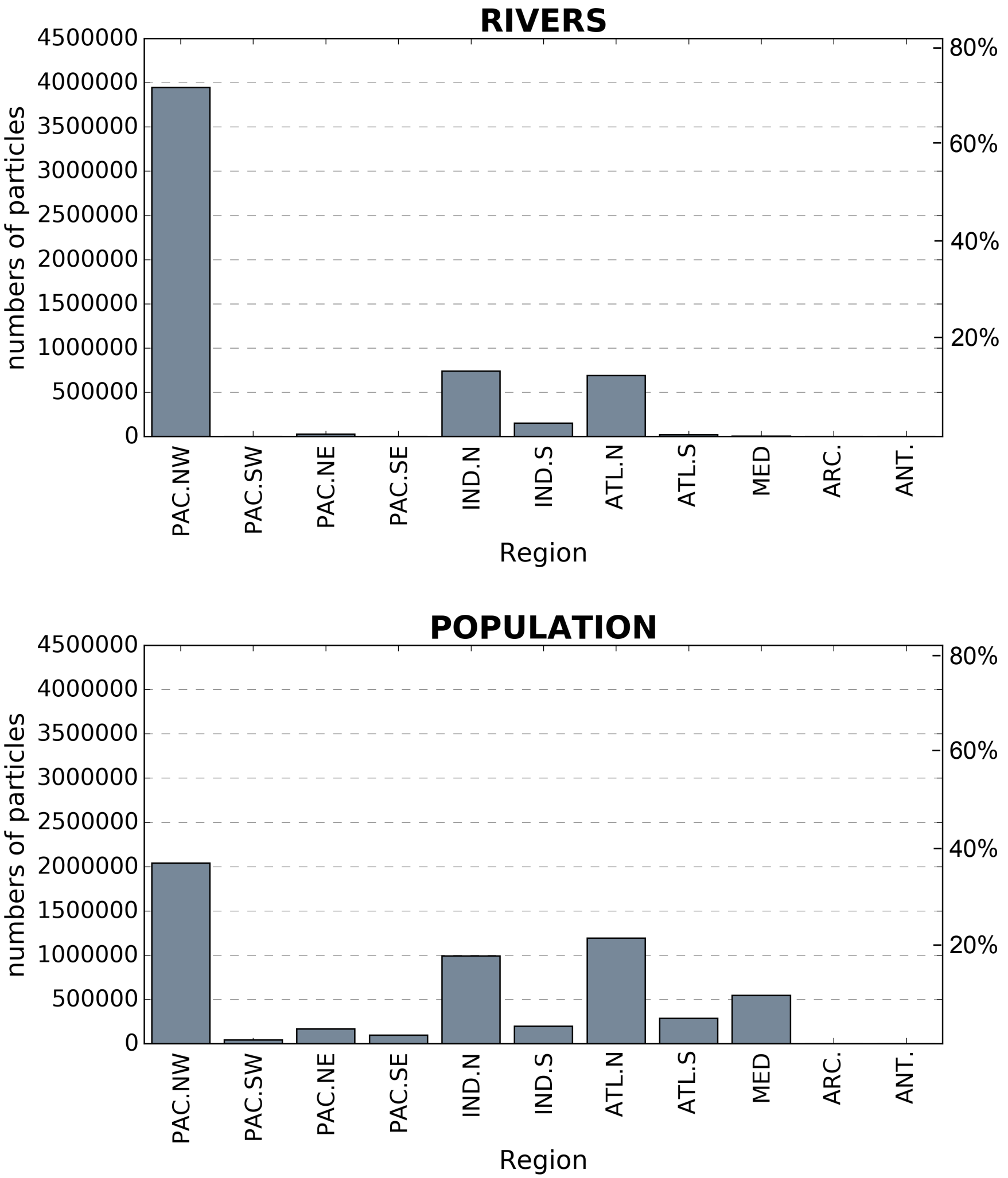

Fig. 1: Total number of particles released in each region in the Lagrangian experiments in the river scenario (top) and the population scenario (i.e., mismanaged waste from the coastal population) (bottom) (maps of the input positions are given in Fig. S1 and oceanic regions are defined in Fig. S2). A total of 5,589,080 and 5,571,720 particles are released in the river and population scenarios, respectively. Percentages on the right are given relatively to the total particles released.

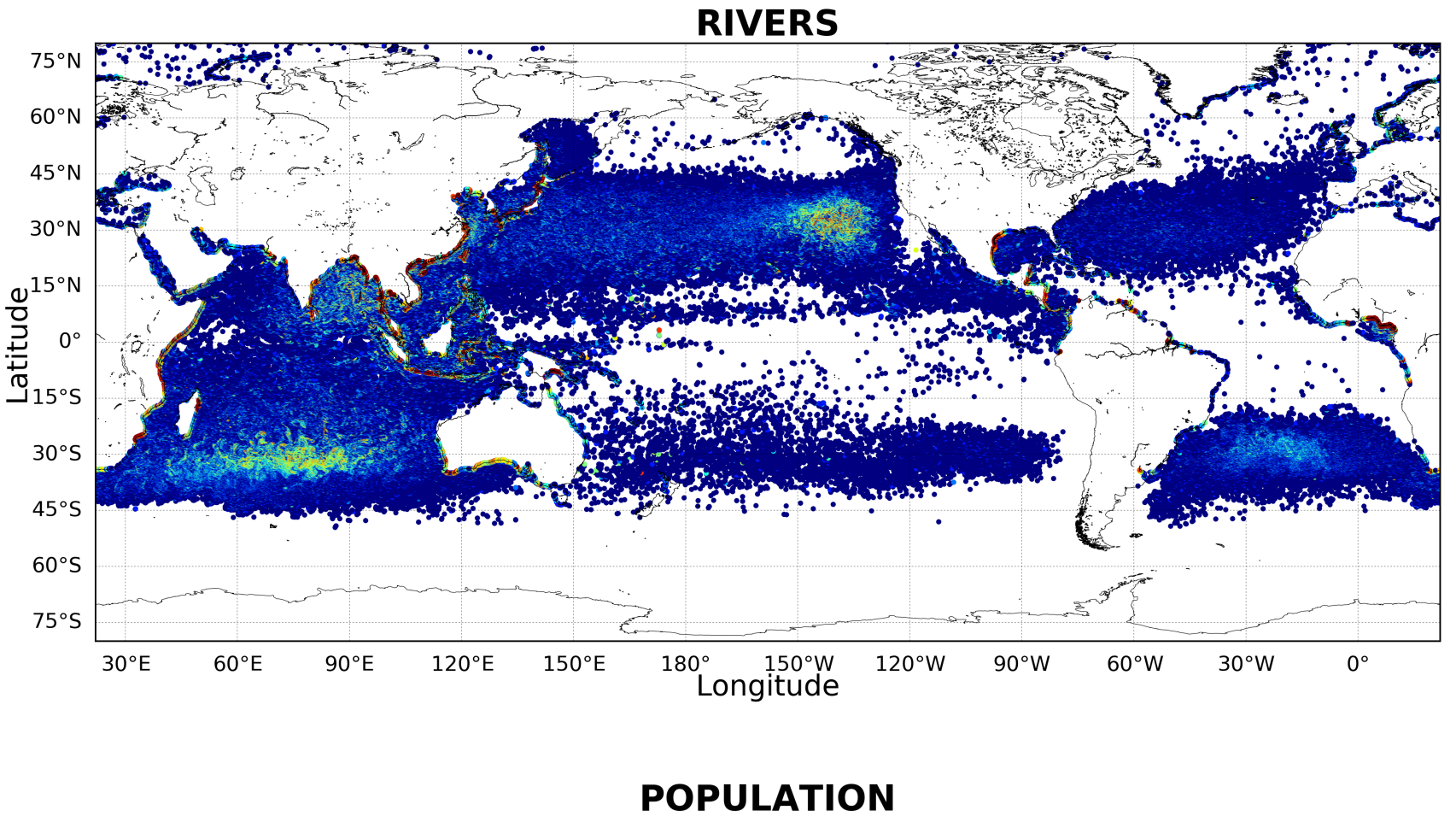

Fig. 2: Number of particles per model grid cell at the end of the model simulations (year 23) in the river scenario (top) and the population scenario (i.e., mismanaged waste from the coastal population) (bottom).

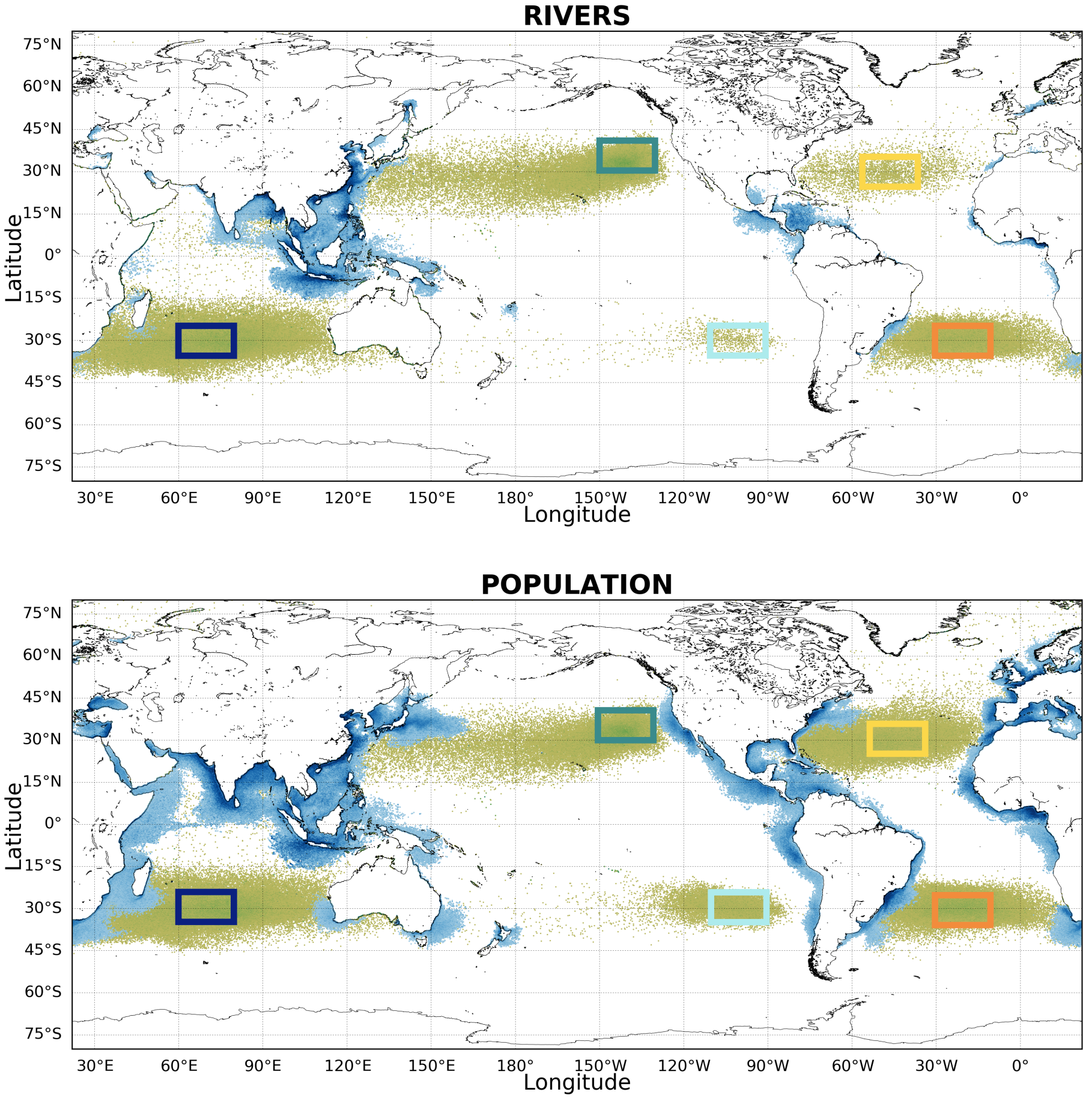

Fig. 3: Number of particles per model grid cell at different ages in the river scenario (top) and the population scenario (i.e., mismanaged waste from the coastal population) (bottom): particles aged 1 month (blue colorbar) and particles aged 22 years (green colorbar). Note that the total number of 1-month-old particles is 22 times higher than the number of 22-year-old particles (released during the first year of the Lagrangian experiment). The colored boxes represent the center of the five main convergence zones (CVZs).

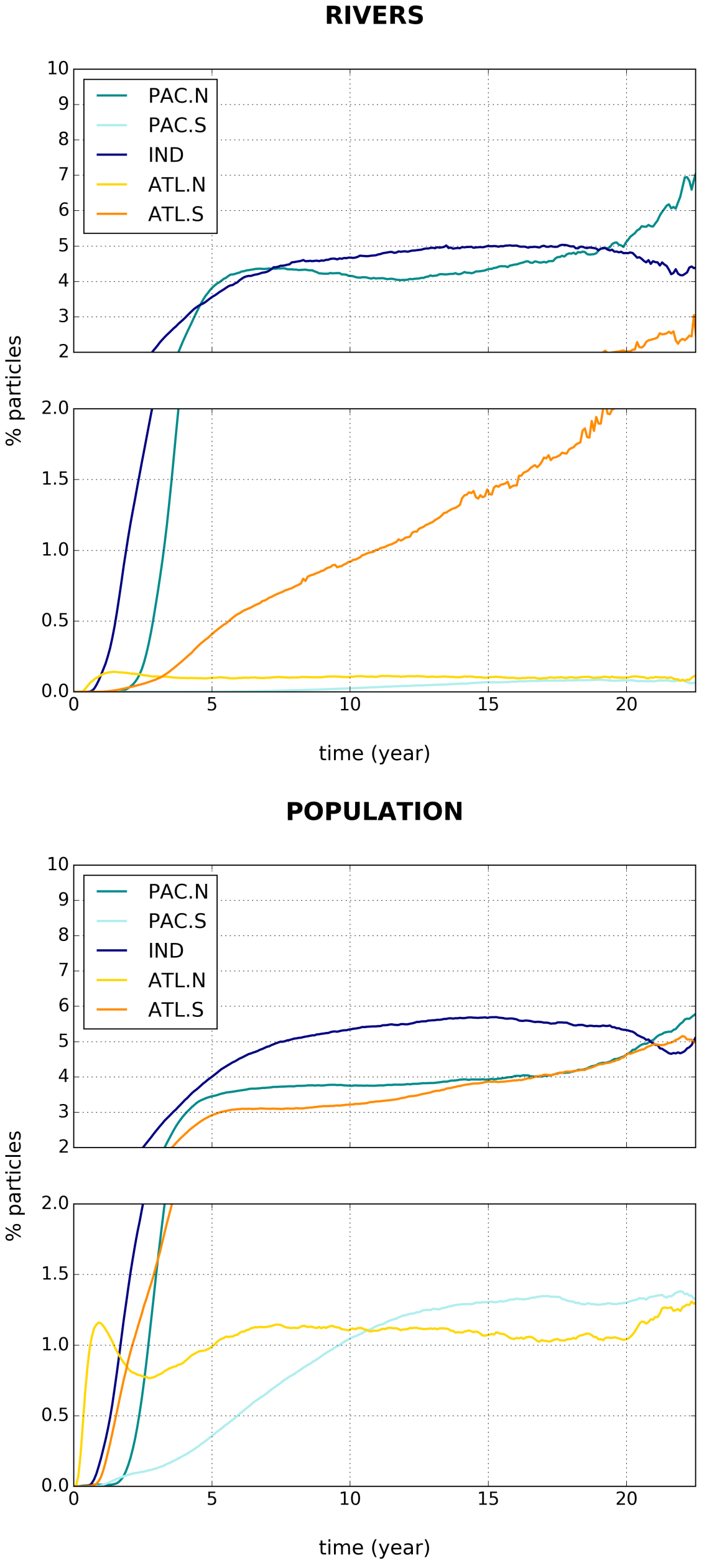

Fig. 4: Percentage of particles in each CVZ center, as a function of simulation time in the river scenario (two upper panels) and the population scenario (i.e., mismanaged waste from the coastal population) (two lower panels). The percentage represents the number of particles in each CVZ normalized by the number of active particles, i.e., the number of particles released at time t since the beginning of the simulation (note that this number of active particles increases each month, as explained in section 2b).

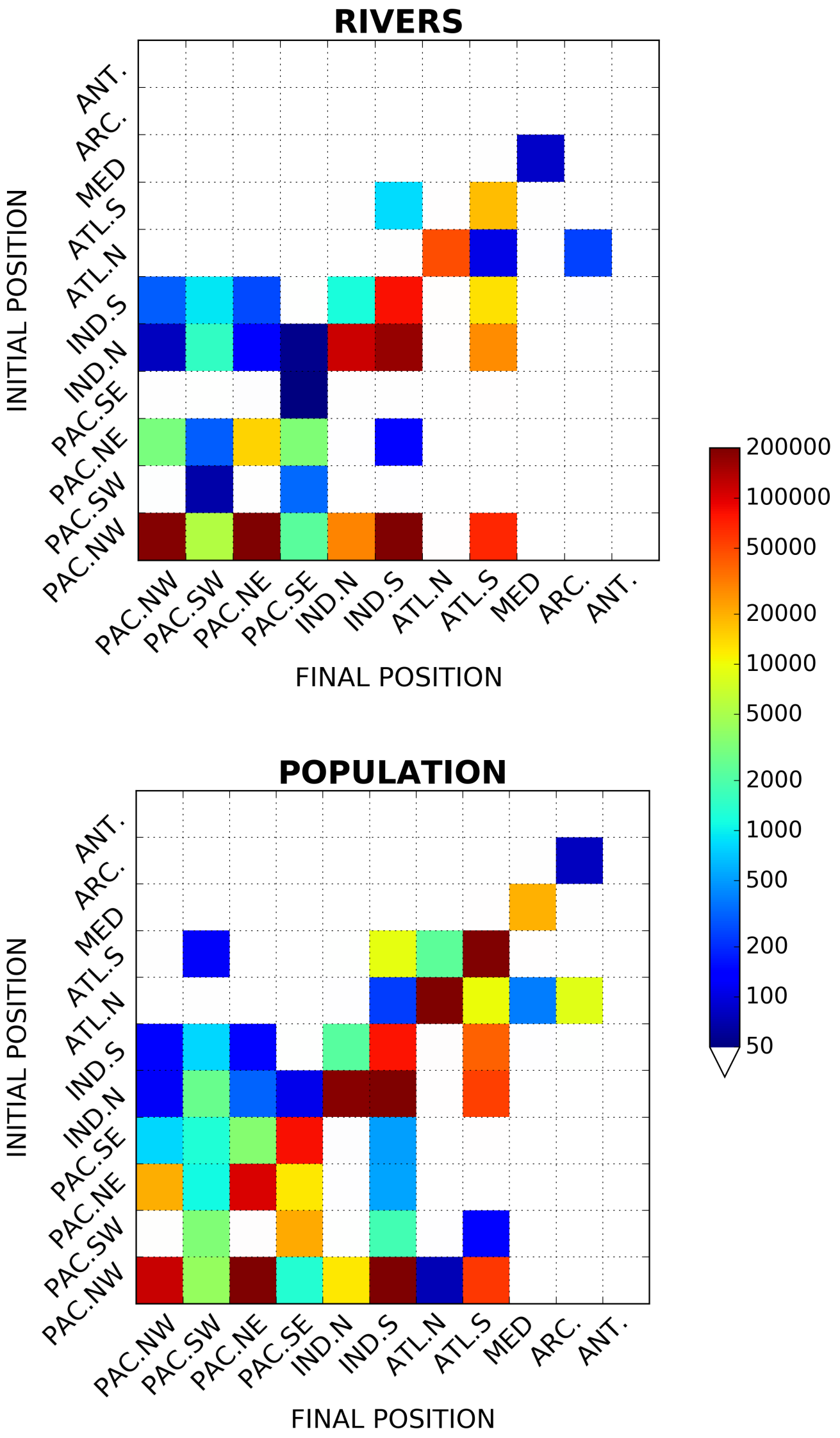

Fig. 5: Connectivity matrix for particles that end up in the sea (case a), in the river (top) and population (i.e., mismanaged waste from the coastal population) (bottom) scenarios. The cells are colored according to the number of particles originating from the region indicated on the y-axis and ending up in the region indicated on the x-axis. White cells indicate low connectivity (fewer than 50 particles).

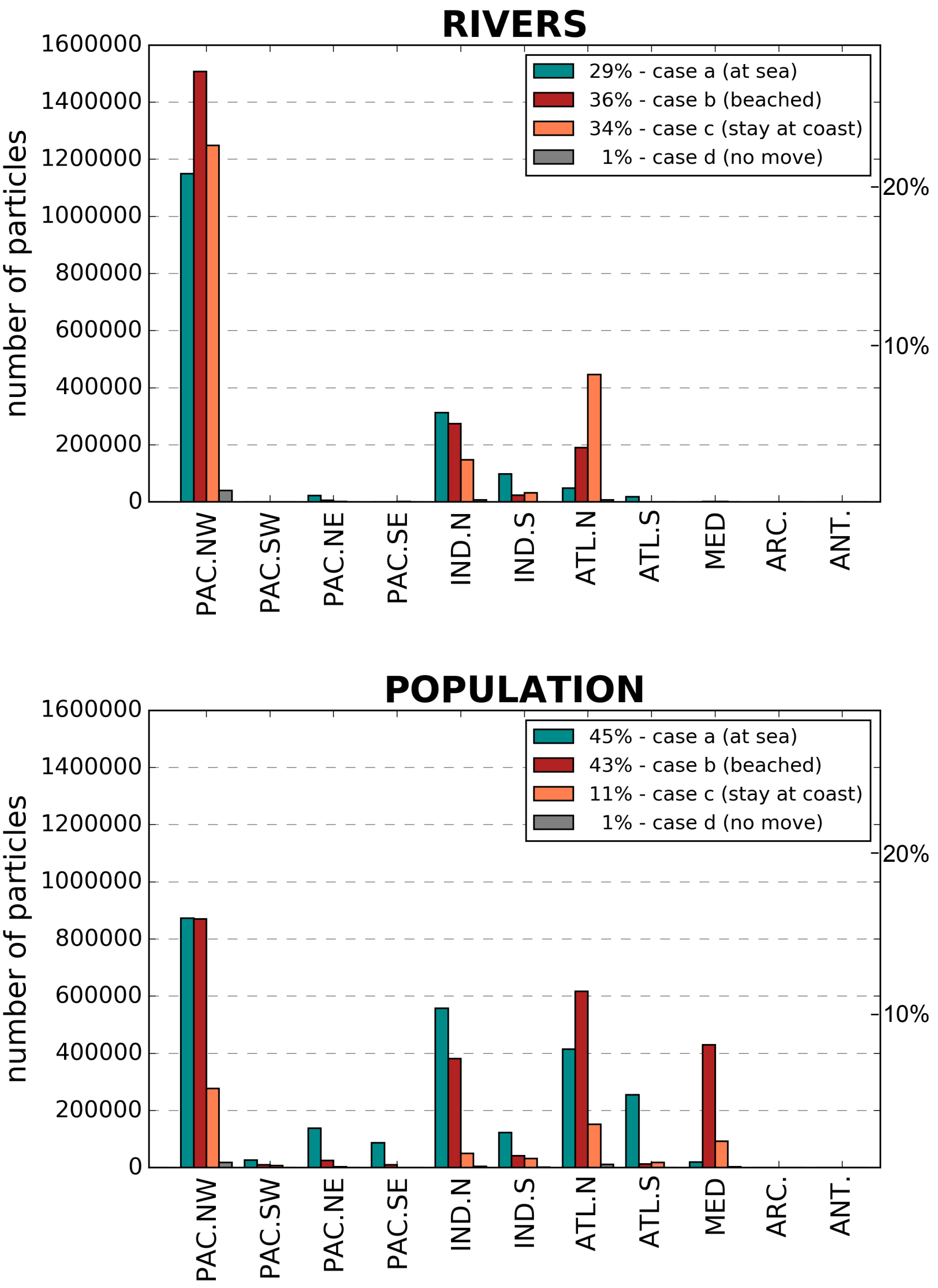

Fig. 6: Histogram of the fates of particles according to their initial region in the Lagrangian experiments (as in Figure 1): particles ending at sea (cases a), beached particles (case b), particles remaining along the coast (case c) or particles that do not move (case d), in the river scenario (top) and the population scenario (i.e., mismanaged waste from the coastal population) (bottom). Percentages on the right are given relatively to the total particles released.

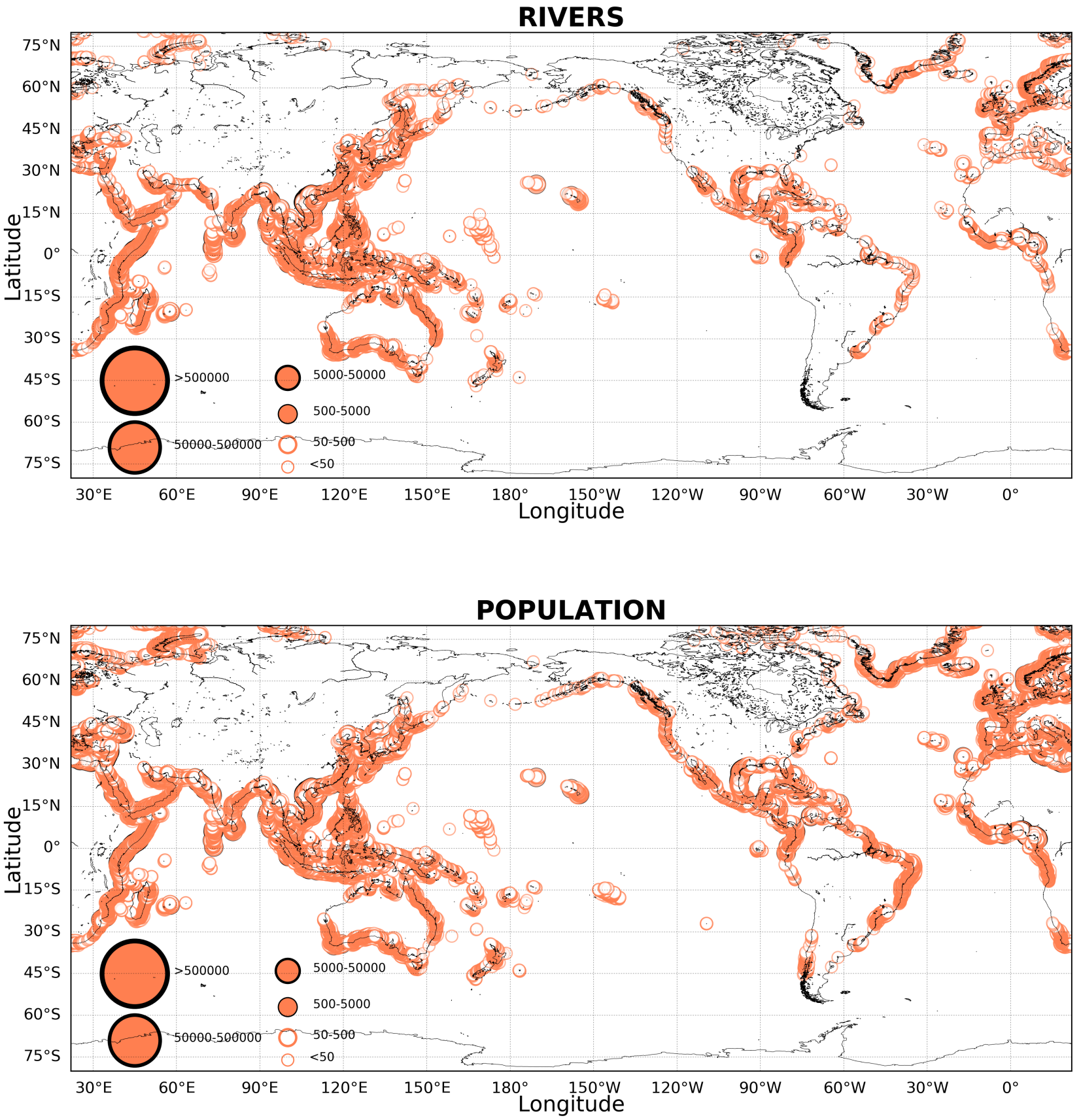

Fig. 7: Number of beached particles (case b) in each coastal grid cell at the end of the simulation (year 23) in the river scenario (top) and the population scenario (i.e., mismanaged waste from the coastal population) (bottom).

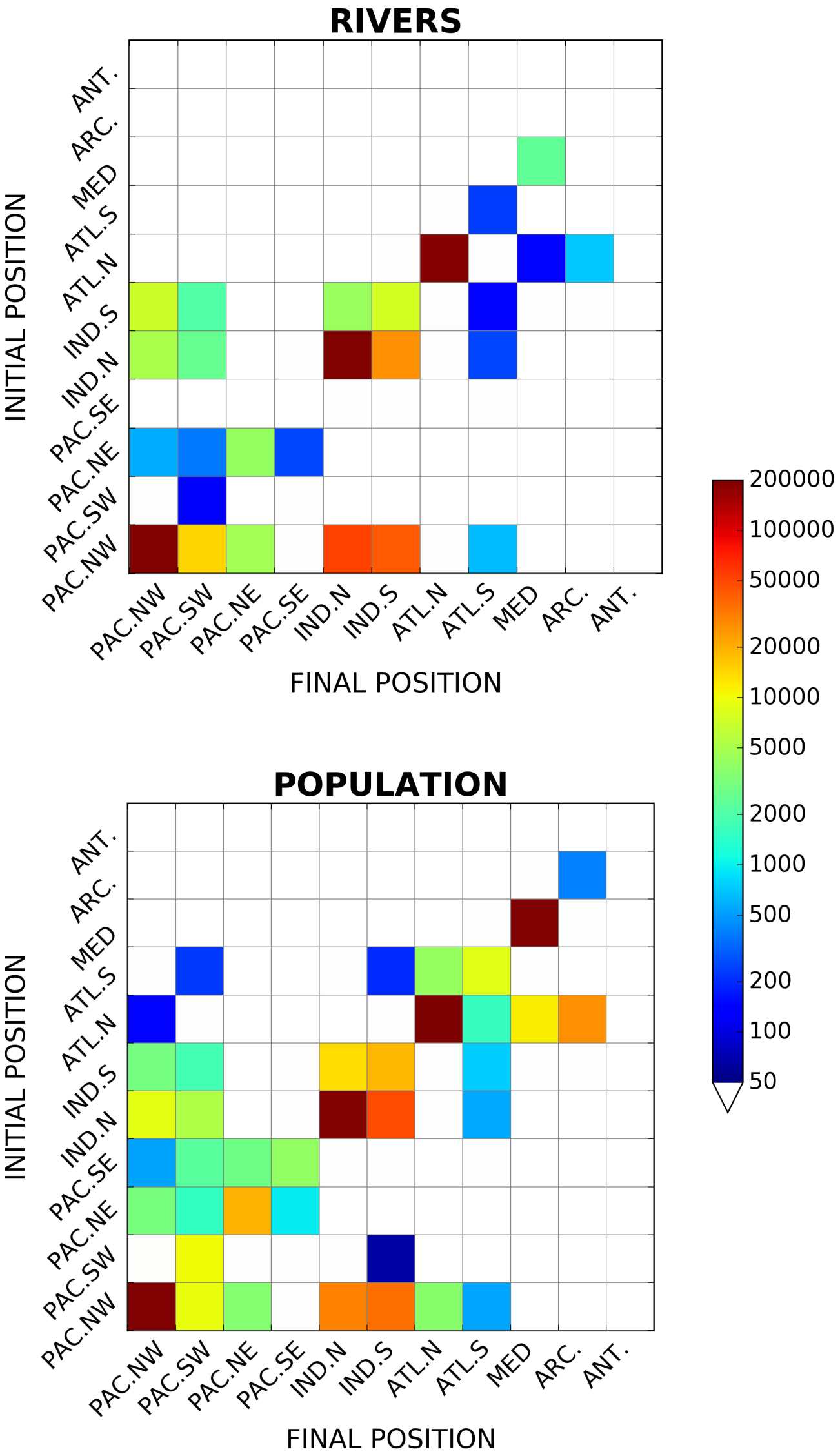

Fig. 8: Connectivity matrix for beached particles (case b) in the river (top) and population (i.e., mismanaged waste from the coastal population) (bottom) scenarios. The cells are colored according to the number of particles originating from the region indicated on the y-axis and ending up in the region indicated on the x-axis. White cells indicate low connectivity (fewer than 50 particles).

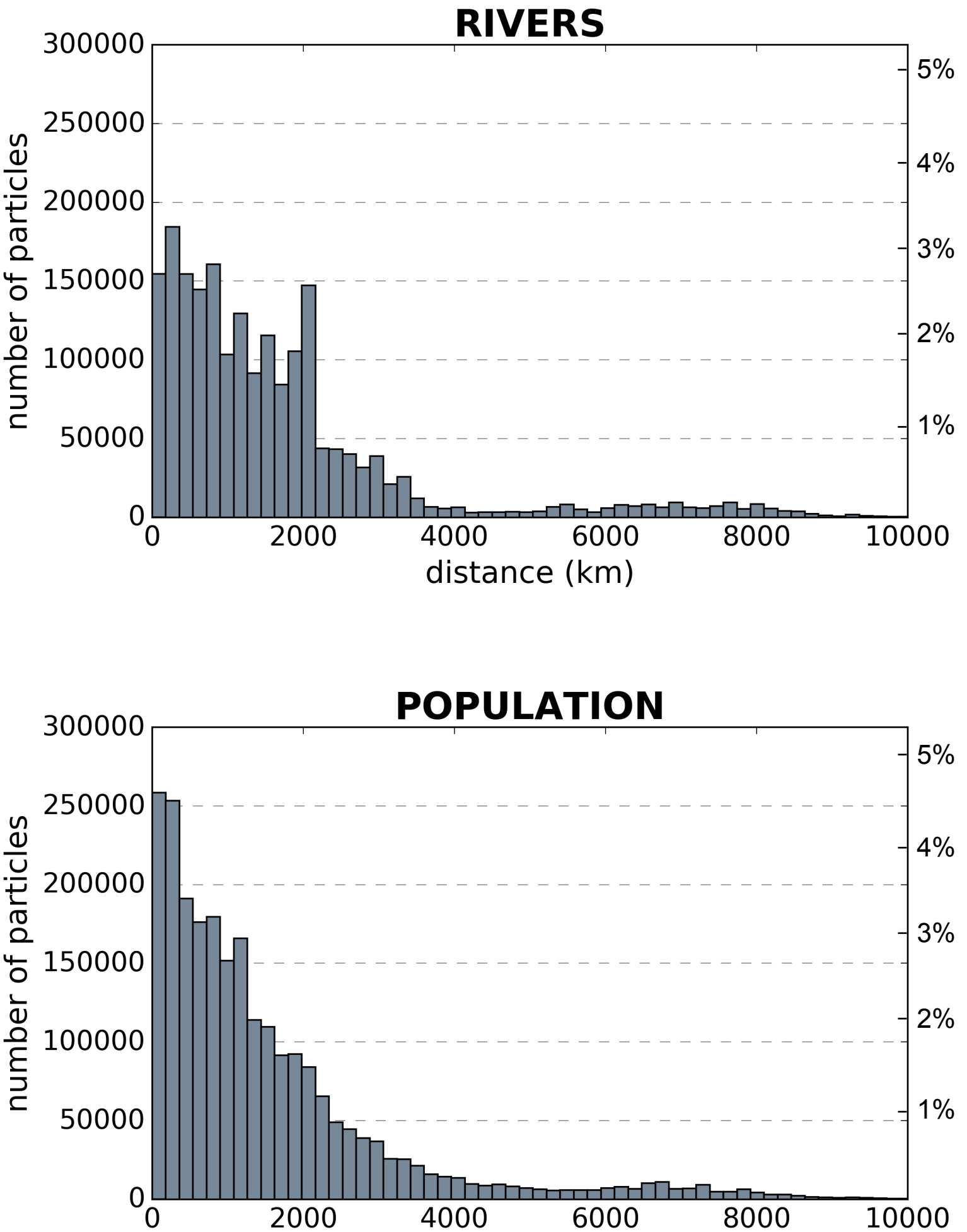

Fig. 9: Histogram of the distances traveled by beached particles (case b) in the river scenario (top, 2,400,151 beached particles in case b) and population scenarios (i.e., mismanaged waste from the coastal population) (bottom, 2,003,808 beached particles in case b). Distances are computed between the initial position and the beached position (see details in section 4). Percentages on the right are given relatively to the total particles released.

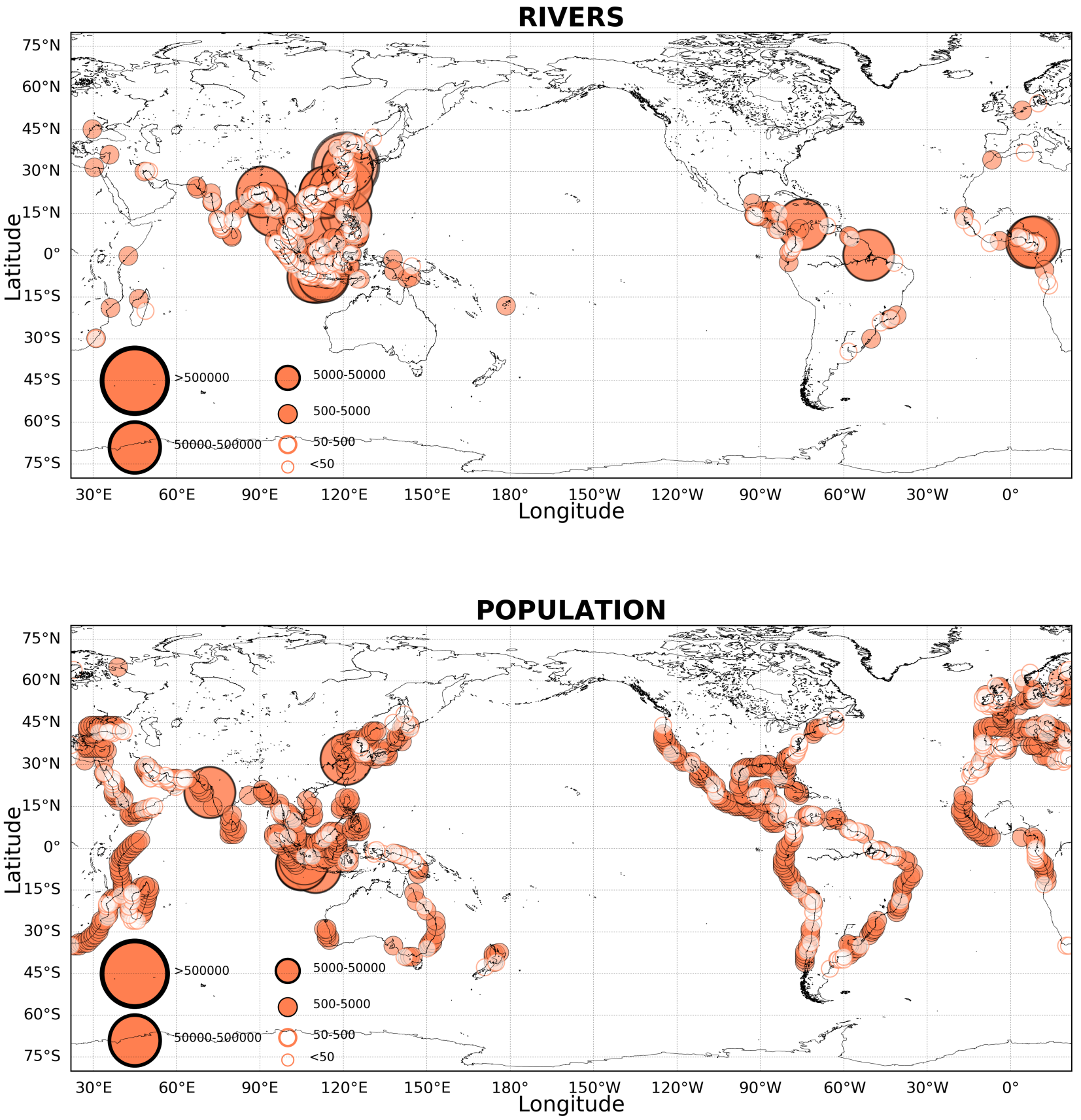

Fig. S1: Number of particles released in each model grid cell in the river scenario (top) and in the population scenario (i.e., mismanaged waste from the coastal population) (bottom). A total of 5,589,080 and 5,571,720 particles are released in the river scenario and the population scenario, respectively.

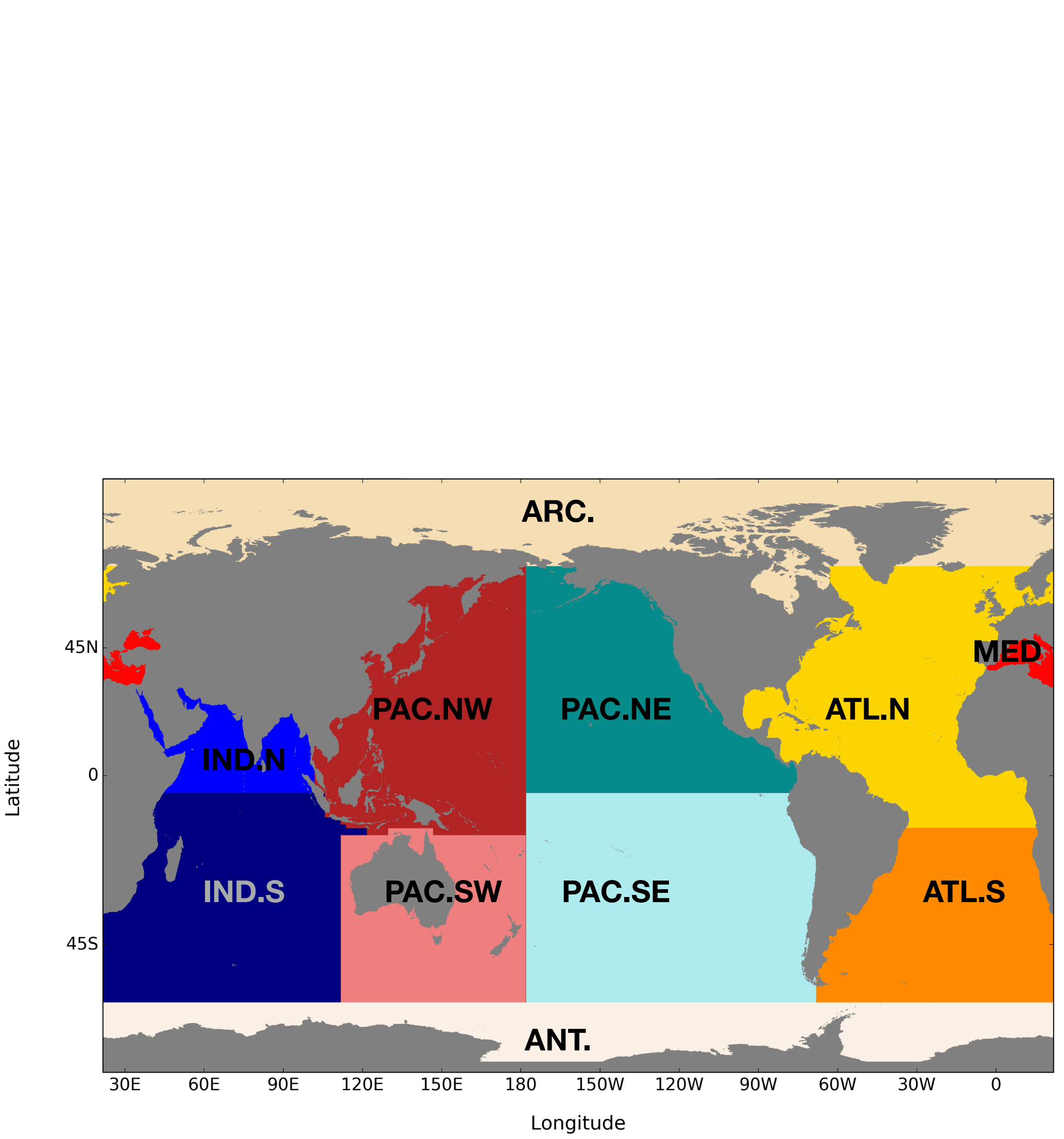

Fig. S2: Definition of the 11 oceanic regions. Note that our definition of the Southwest Pacific actually represents Oceania, and includes the extreme eastern Indian Ocean.

RIVERS

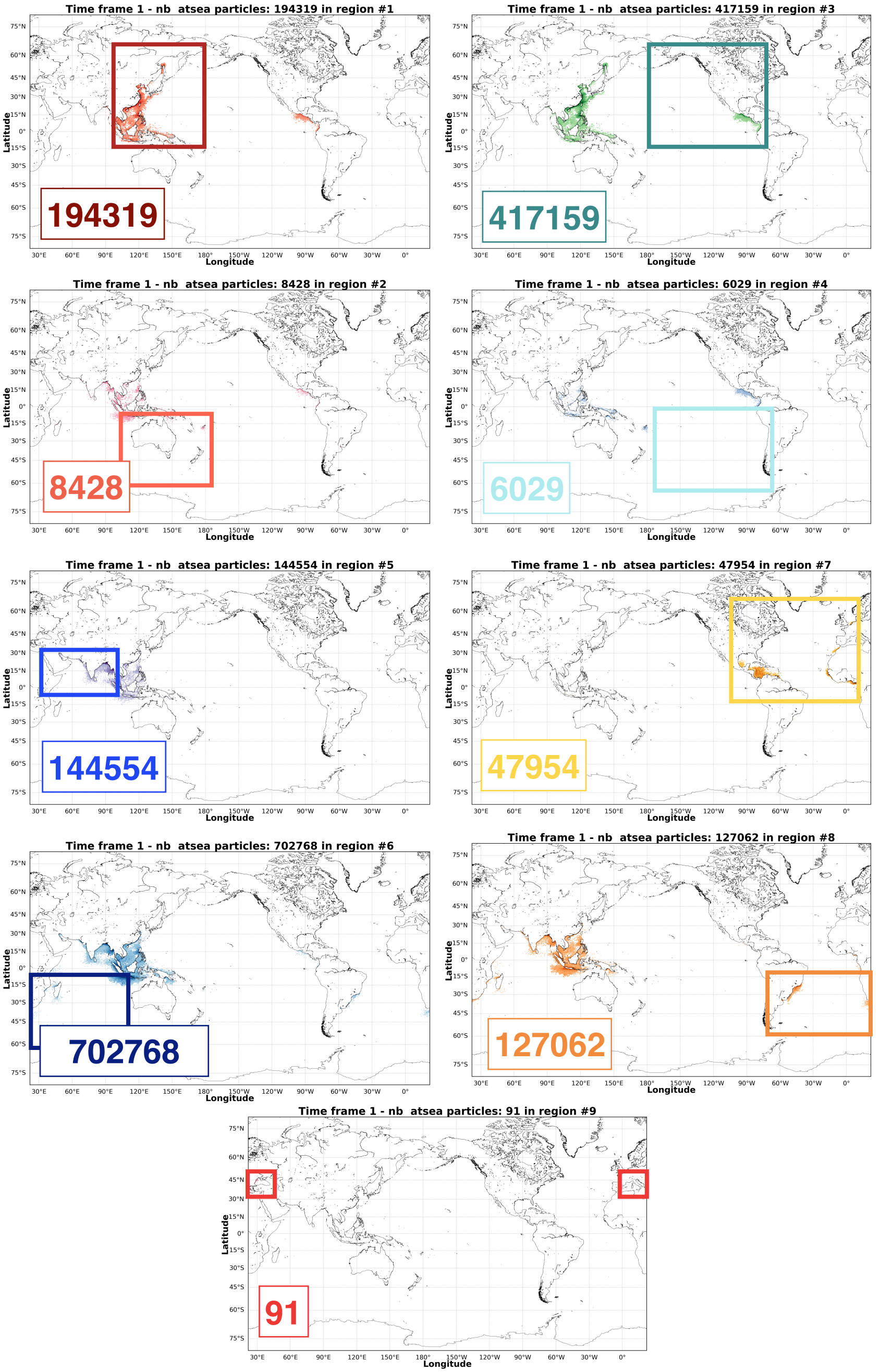

Fig. S3: Near-initial position (1-month after release) of particles ending at sea (case a) in the different oceanic regions in the river scenario. The number of particles is given in the lower left box for each panel.

POPULATION

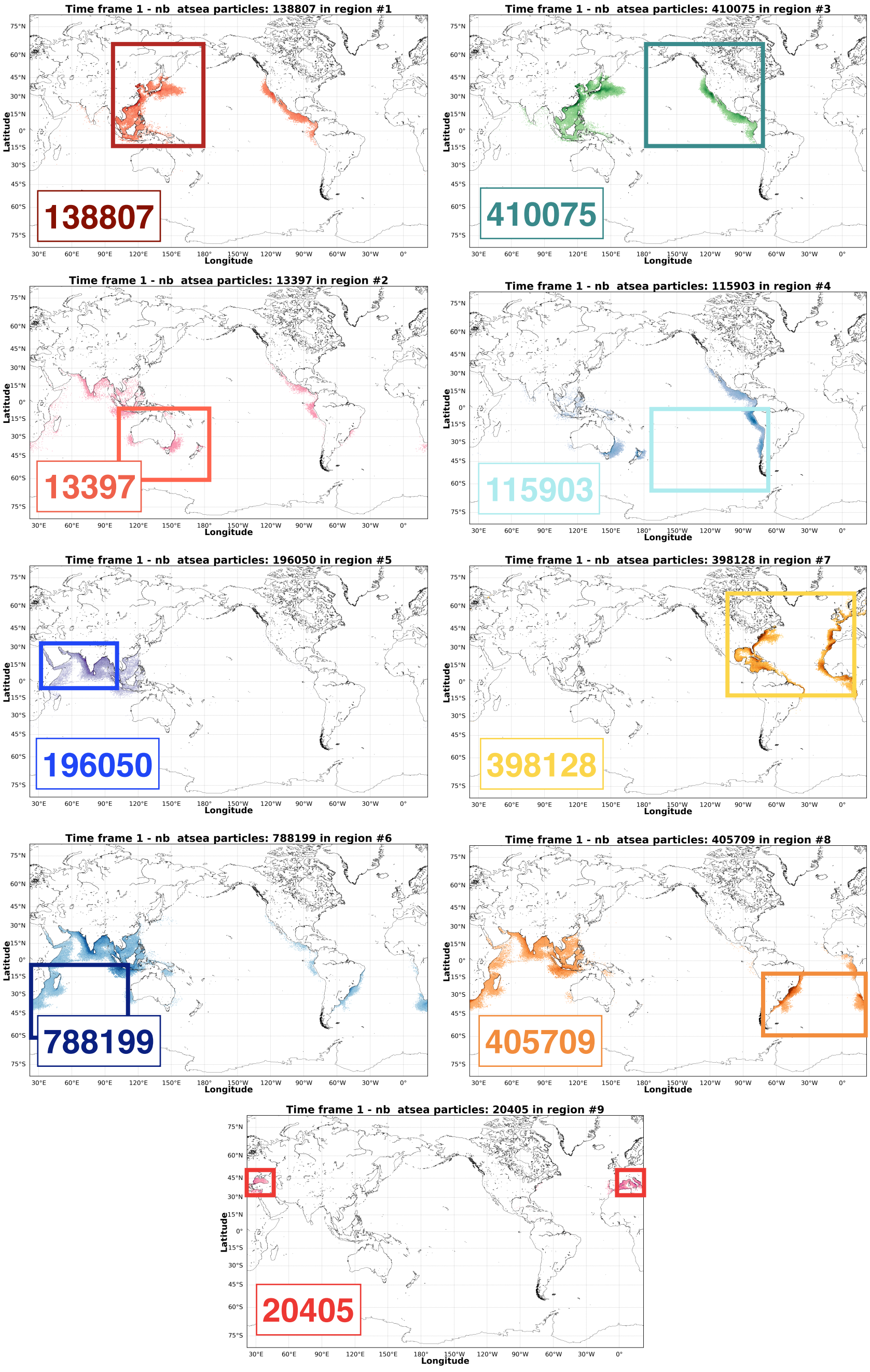

Fig. S4: Near-initial position (1-month after release) of the particles ending at sea (case a) in the different oceanic regions in the population scenario (i.e., mismanaged waste from the coastal population). The number of particles is given in the lower left box for each panel.

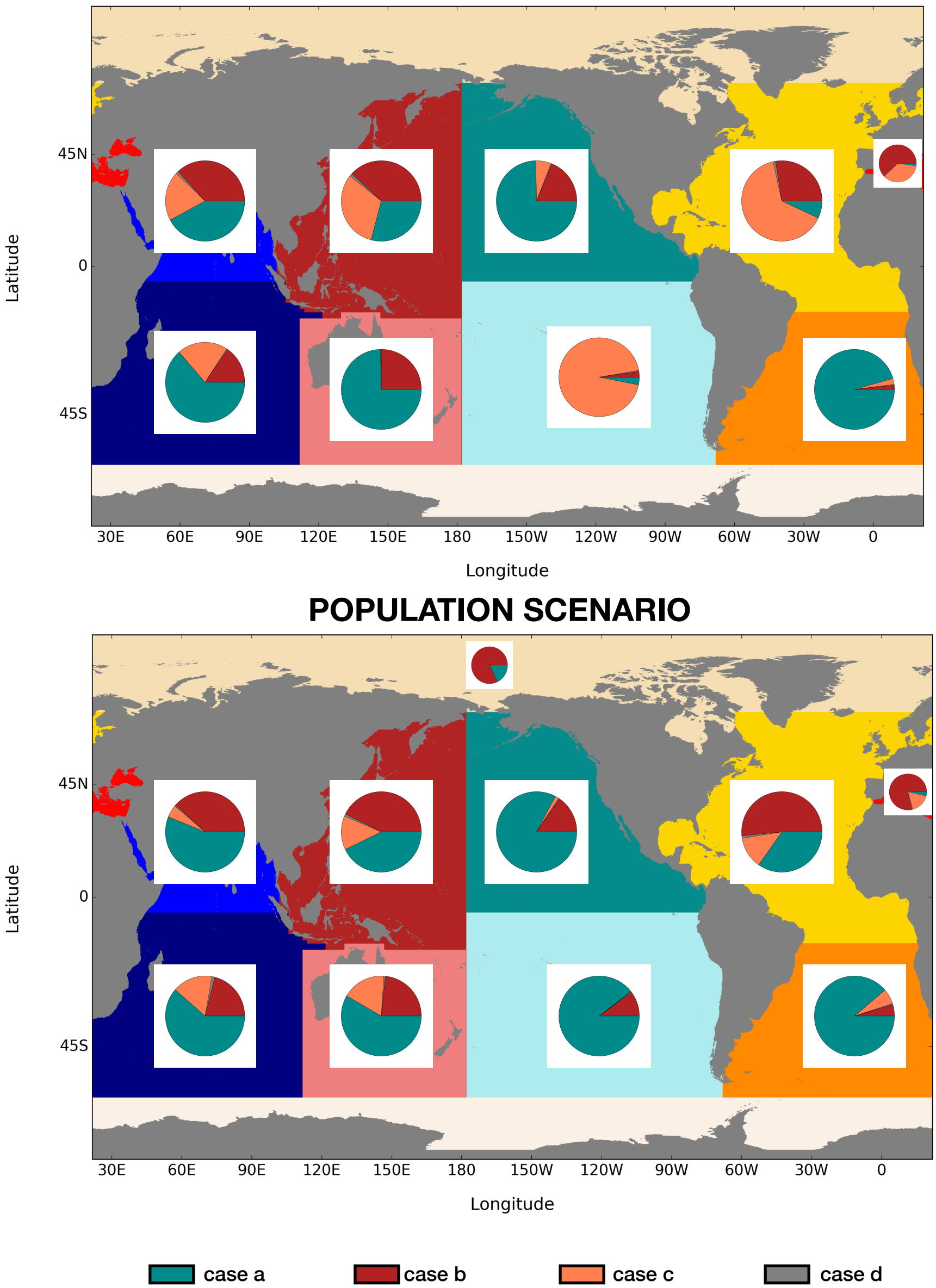

Fig. S5: Pie chart of the fate of particles in cases a (particles ending at sea, in green), b (beached particles, in red), c (particles remaining along the coast, in orange) and d (particles that do not move, in gray) as a function of their initial position in the different oceanic regions (defined in Fig. S2) in the river scenario (top) and the population scenario (i.e., mismanaged waste from the coastal population) (bottom).

RIVERS

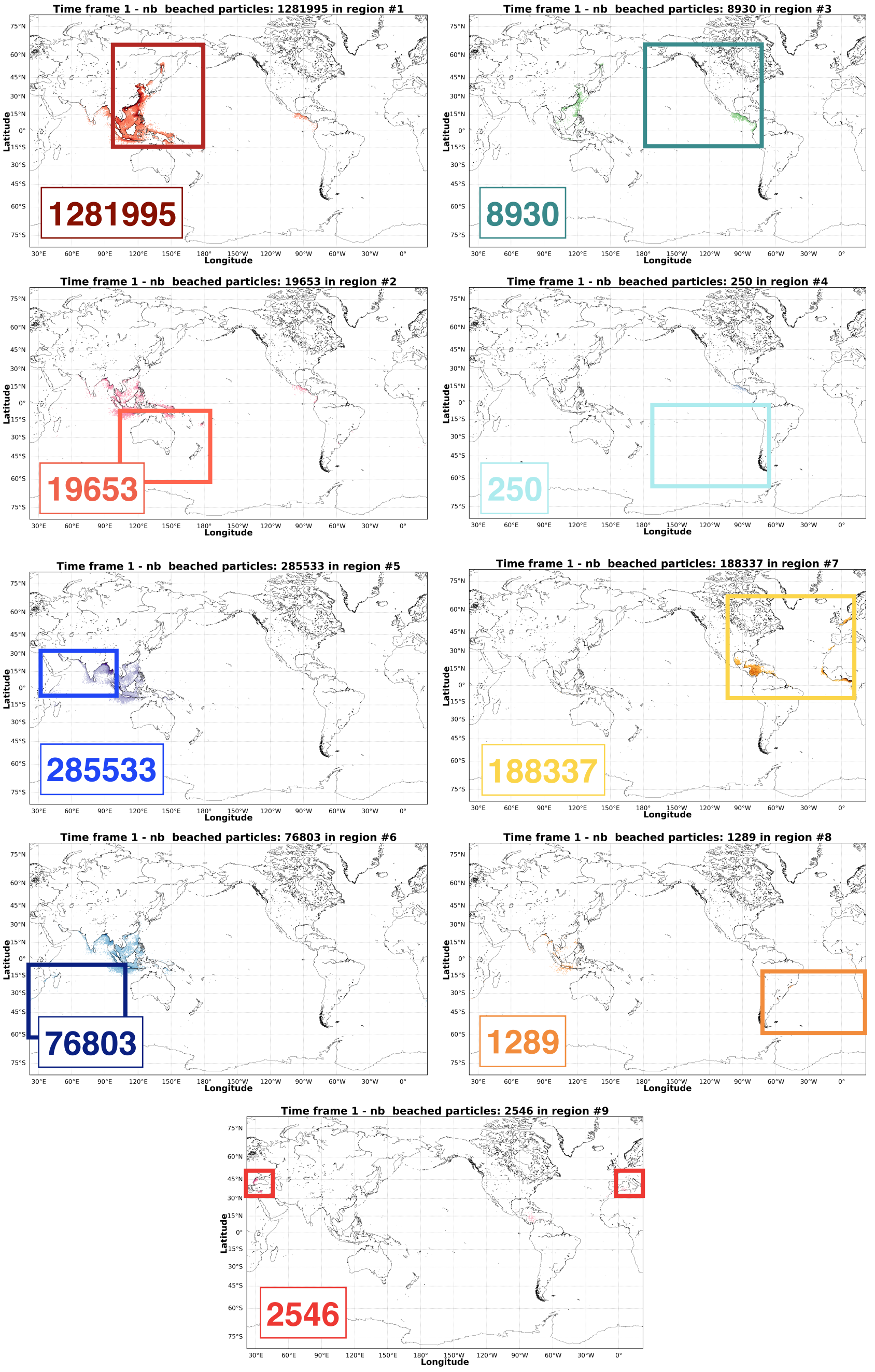

Fig. S6: Near-initial position (1-month after release) of the beached particles (case b) in the different oceanic regions in the river scenario. The number of particles is given in the lower left box for each panel.

POPULATION

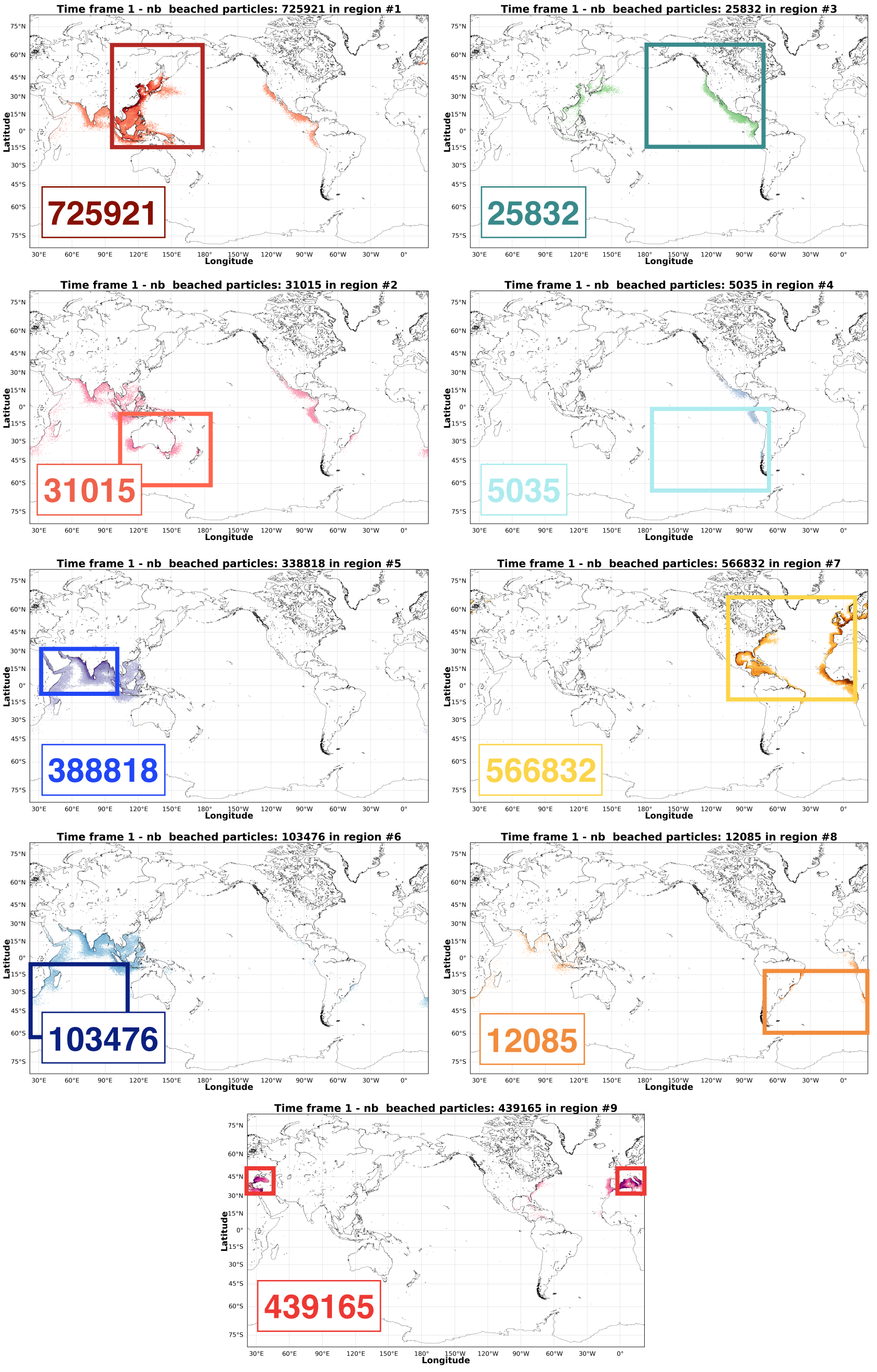

Fig. S7: Near-initial position (1-month after release) of the beached particles (case b) in the different oceanic regions in the population scenario (i.e., mismanaged waste from the coastal population). The number of particles is given in the lower left box for each panel.

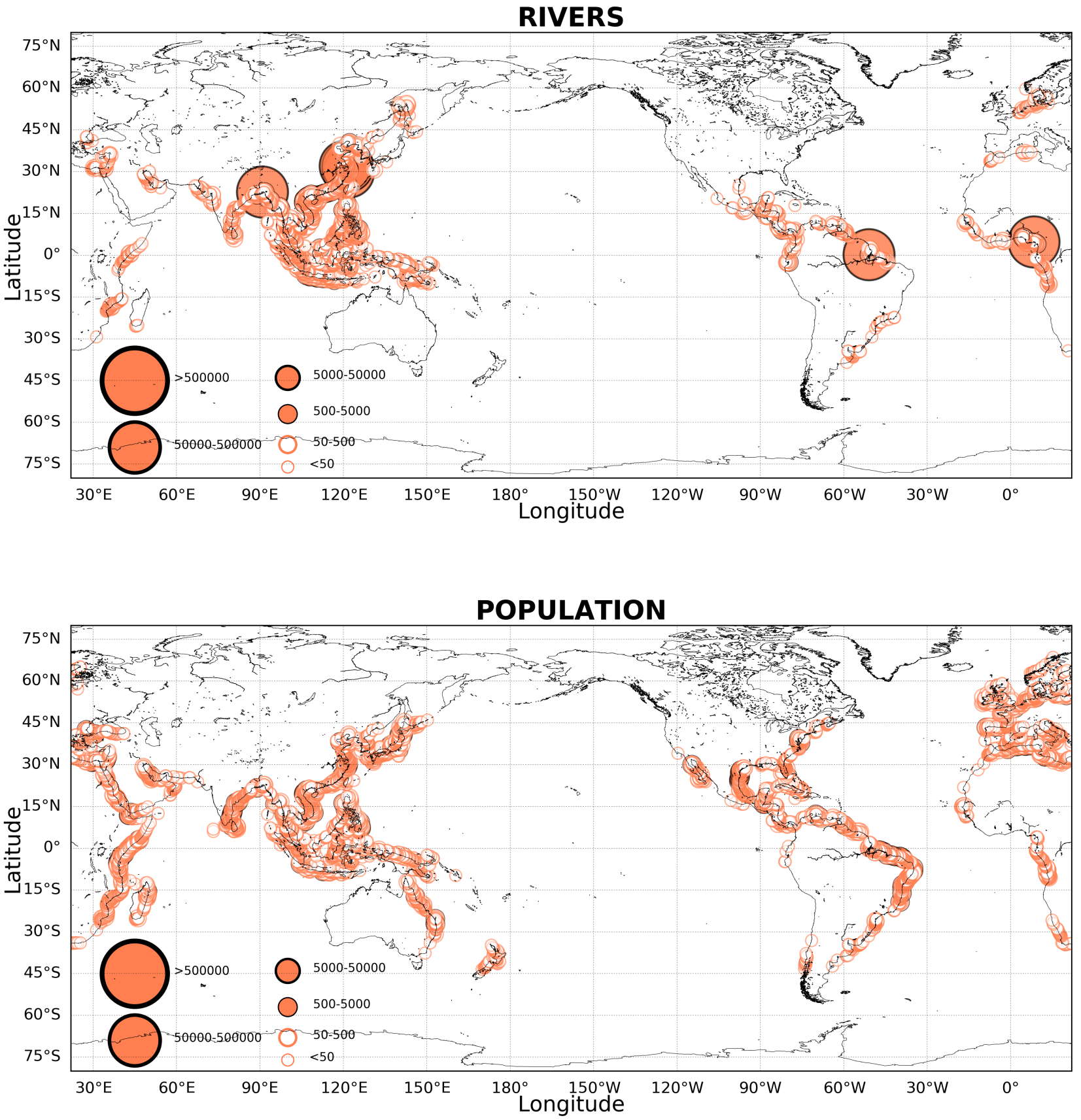

Fig. S8: Number of particles remaining on the shore (case c) in each coastal grid cell at the end of the simulation (year 23) in the river scenario (top) and the population scenario (i.e., mismanaged waste from the coastal population) (bottom).

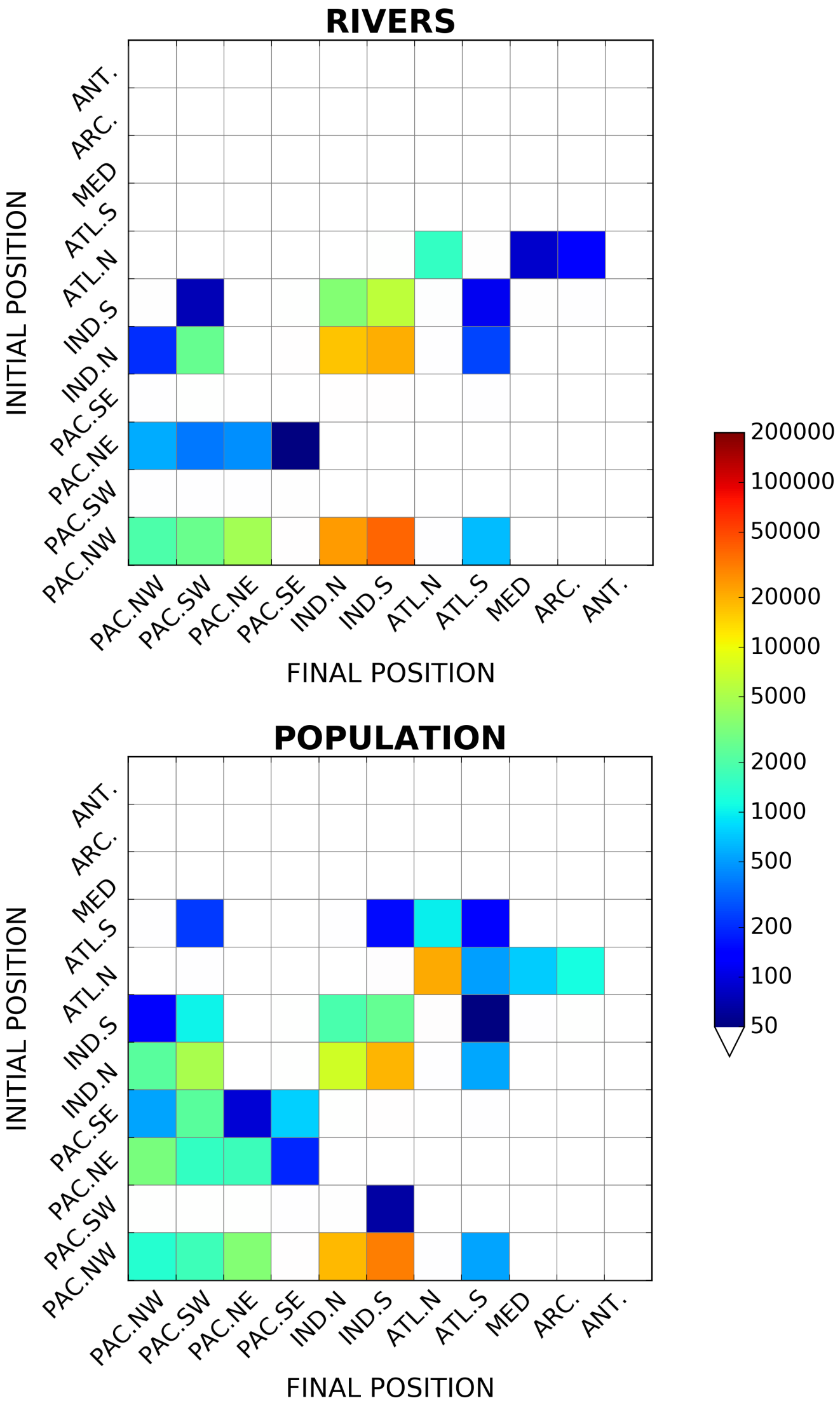

Fig. S9: Connectivity matrix for beached particles that have traveled a long distance, i.e., >5000 km (sub-selection from case b) at the end of the simulation (year 23) in the river (top) and population (bottom) scenarios. Cells are colored according to the number of particles originating from the region indicated on the y-axis and ending up in the region indicated on the x-axis. White cells indicate low connectivity (fewer than 50 particles).